# MASTERARBEIT | MASTER'S THESIS

Titel | Title

Investigation of natural products for their anti-inflammatory potentials in relevant cell culture models

verfasst von | submitted by

Janvi Mahi BSc

angestrebter akademischer Grad | in partial fulfilment of the requirements for the degree of

Magistra pharmaciae (Mag. pharm.)

Wien | Vienna, 2025

| | |
|---|---|
| Studienkennzahl lt. Studienblatt \| Degree programme code as it appears on the student record sheet: | UA 066 605 |
| Studienrichtung lt. Studienblatt \| Degree programme as it appears on the student record sheet: | Masterstudium Pharmazie |
| Betreut von \| Supervisor: | Univ.-Prof. Dr. Verena Dirsch |
| Mitbetreut von \| Co-Supervisor: | Mag. Dr. sc. ETH Alexander Franz Perhal |

## Abstract

G-protein coupled receptors (GPCR) are responsible for a wide range of physiological and pathological responses. They are activated by extracellular stimuli and trigger an intracellular signaling pathway mediated through G-proteins and second messengers such as cAMP. Besides influencing various functions such as expression and secretion of proteins, terminating cell responses, enhancing gut microbiota, and many more, their dysregulation could cause inflammatory diseases. Due to the increasing interest in this receptor type, an extensive number of studies have been conducted focusing on the role of GPCRs in inflammation and investigating their potential as therapeutic targets. [1–3]

Because of the complexity of the interaction of GPCRs in inflammation, this thesis focused on two GPCRs, TGR5 and GPR84. These receptors are expressed on macrophages and neutrophils, which are components of the innate immune system. The aim was to identify potential ligands from the DNTI project that influence these receptors and could potentially lead to decreased inflammatory responses. Various cell-based assays, such as CRE-Luciferase, EPAC, and PMN migration assays, were conducted to test the effects of compounds on TGR5 and GPR84.

## Zusammenfassung

G-Protein gekoppelte Rezeptoren (GPCR) sind für eine Großzahl von pathologischen und physiologischen Reaktionen verantwortlich. Ihre Aktivität wird eingeleitet über einen extrazellulären Stimuli, der eine intrazelluläre Signalkaskade auslöst. Diese wird über das cytosolische G-Protein und Sekundärbotenstoffe, wie cAMP, übermittelt. Dieser Rezeptortyp beeinflusst verschiedenste Funktionen, unter anderem die Expression von bestimmten Genen, Sekretion von Proteinen und Beendigung von Zellsignalen. Jedoch kann dessen Dysregulation entzündliche Erkrankungen auslösen. Aufgrund des zunehmenden Interesses an dieser Rezeptorklasse wurde eine Vielzahl von Studien durchgeführt. Damit wurde die Rolle der GCPRs in Entzündungen und deren therapeutische Relevanz untersucht. [1–3]

Die Komplexität und Vielseitigkeit in der Beziehung zwischen GCPRs und entzündlichen Erkrankungen führten dazu, dass der Fokus dieser Arbeit auf zwei unterschiedlichen Rezeptoren lag. TGR5 und GPR84 sind G-Protein gekoppelte Rezeptoren, die von Makrophagen und neutrophilen Granulozyten exprimiert werden. Sie können die Freisetzung von proinflammatorischen Mediatoren modulieren und Zellmigration in entzündetes Gewebe beeinflussen. [4,5]

Das Ziel war es, Liganden aus dem DNTI-Projekt zu identifizieren, die die Rezeptoraktivität beeinflussen und dadurch potenziell eine Reduktion der Entzündungsreaktionen bewirken könnten. Die Effekte, der untersuchten Substanzen, auf TGR5 und GPR84 wurden mithilfe unterschiedlicher zellbasierter Assays (CRE-Luciferase, EPAC und PMN-Migration Assay) bestimmt.

## Acknowledgement

Firstly, I would like to express my sincere gratitude to Univ.-Prof. Dr. Verena Dirsch for providing me with the opportunity to work on my master's thesis in the Molecular Targeting Group of the Division of Pharmacognosy at the University of Vienna. I was able to deepen my understanding of molecular interactions with natural products, gain insight into laboratory work ethics and reflect on future career paths. These experiences allowed me to increase my interest in pharmacognosy.

I would also like to thank Mag. Dr. Alexander Perhal for his invaluable guidance and support in the laboratory and during the writing process. His expertise, patience and insightful critique enriched my experience with this group.

I am also grateful to the entire AKDirsch group, who welcomed me with open arms and supported me during the practical part of my thesis. I will always appreciate their openness and willingness to help, which created a comfortable and encouraging atmosphere.

Lastly, I want to thank my family and friends for their unwavering support and constant encouragement throughout my studies. They made even the most difficult times manageable.

# Table of Contents

# A. Introduction

## 1. Immune system

The immune system is an essential part of the human body. Without it no barrier stands against the invasion of bacteria, viruses or parasites and the following infections and diseases. The immune system is divided into two parts the innate and the adaptive immune system (**Figure 1**). However, due to their constant interactions, distinguishing them as two separate divisions of the immune system is often difficult and not meaningful. [6,7]

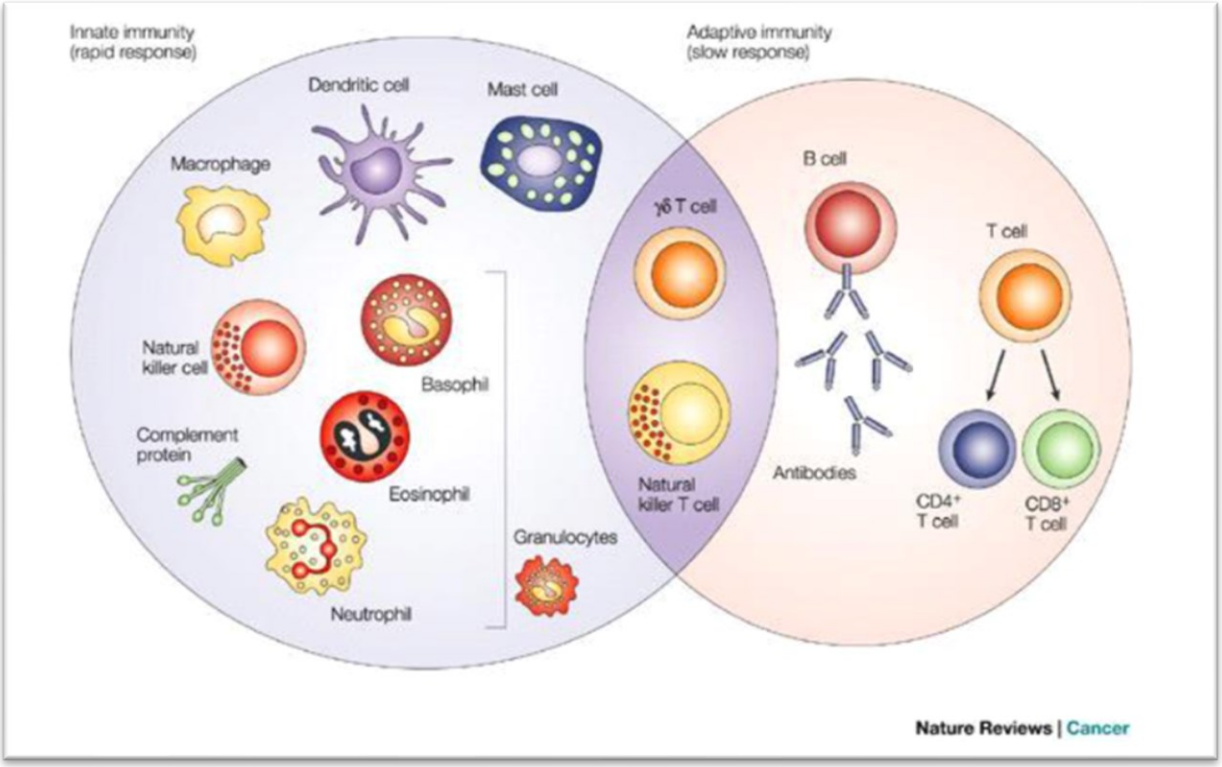


**Figure 1**. *Schematic overview of the innate and adaptive immune system. Illustration taken from Nature Reviews Cancer 2004;4,11-22 [7]*
The innate immunity, which is the rapid response to pathogens, consists of mast cells, dendritic cells, macrophages, natural killer cells, complement system and granulocytes. Meanwhile, the adaptive immunity consists of B- and T-cells. These two parts overlap, e.g. through natural killer cells and γδ T-cells. [7]

### 1.2 Innate immunity

The innate immune system provides a general defense as its main function is to distinguish foreign structures from endogenous elements. This is achieved through recognition of pathogen-associated molecular patterns (PAMPs) with pattern recognition receptors (PRR) or discerning missing molecules, which are typically expressed on

normal and healthy cells. However, it lacks the ability for specific antigen recognition and immune responses needing further assistance of adaptive immunity. [8–10]

The innate immune system consists of phagocytes (neutrophils and macrophages), natural killer cells, dendritic cells (DC) and the complement system (**Figure 1**). [10] This initial immune response is triggered by the interaction with pathogens. For instance, macrophages engulf invading microorganisms after contact and release cytokines such as Interleukin-1 (IL-1) and Interleukin-6 (IL-6), needed for cellular communication. These chemical messengers recruit more immune cells, like neutrophils, from the blood stream toward the site of infection/injury to aid in fighting off the foreign organism. In addition, they increase the production of adhesion molecules on endothelial cells so that more immune cells stick to the surface of endothelial cells for easier migration into tissue. The neutrophils secrete more inflammatory mediators upon arrival at the infection site further promoting inflammation. [10–13] Should the innate immunity not be able to fend off the infection, antigen-presenting cells (APC) such as dendritic cells travel toward lymph nodes in which T- and B-cells lie dormant. There the APCs present the antigens and stimulate the lymphocytes, and the adaptive immune response is induced. [6,11]

## 1.2 Adaptive immunity

When the innate immunity does not suffice to rid the body of the infection, the specific immune system is stimulated to aid in the defense. This begins in the lymph nodes with the activation of naïve T cells through APCs, whereas B cells are activated directly through contact with soluble antigens. These lymphocytes then proceed to proliferate and differentiate into their respective effector forms. [6]

Naïve mature T cells are stimulated through APCs upon interaction of the MHC/antigen-peptide complex with the T cell receptor (TCR). However, this signal alone is not enough to activate T cells. A co-stimulation of CD28 is necessary to initiate the differentiation and proliferation processes for these lymphocytes. The ligands (CD80 and CD86) for CD28 are expressed on the surface of mature DCs. This ensures that the immature DCs do not induce inflammatory responses. After the 2-step activation process, T cells differentiate, depending on the expression of $CD4^+$ or $CD8^+$ on their surface, either into helper T- cells (Th1, Th2, Th17 and Treg) or cytotoxic T- cells. T helper cells aid in antibody response by inducing B cell proliferation and differentiation and enhancing phagocytosis through

macrophage activation. In contrast, cytotoxic T cells show a direct approach of killing virus-infected host cells by inducing apoptosis. [10,11,14]

Naïve mature B-cells activation is induced through two pathways: T-cell-independent or -dependent. The T-cell-independent pathway is triggered when antigens, with repetitive epitopes, cross-link multiple B cell receptors (BCRs). Even though the B cells are activated, they are not able to undergo isotype-switch or differentiation without T helper cells, thus only expressing low-affinity IgMs (Immunoglobulin M). First, the B cells bind an antigen with their BCR and internalize the receptor/antigen complex. After processing the antigen intracellularly, the cells present the remnants with MHCII molecules on their surface. When a T helper cell recognizes this antigen-MHCII complex via its T cell receptor (TCR), they link to B cells. Their interaction leads to the temporary expression of CD40L on the T cell, which binds to CD40 on B cells. In addition, T helper cells release cytokines such as IL-5 and IL-4 to enhance the activation process. This interaction triggers a rapid proliferation of B cells, resulting in the formation of germinal centers in the lymph nodes. Within these centers proliferation and differentiation processes are conducted, including class-switch and somatic hypermutation. The activated B cells differentiate into plasma and memory cells. The latter are selected based on the affinity of their antibodies to the presented antigen, ensuring a more rapid reaction during a second exposure to the same pathogen. Thus, developing immunological memory and specificity. [10,14,15]

The adaptive immunity is not only responsible for generating a specific immune response but also lays the foundation for a variety of therapeutically relevant applications. For instance, insights gained from antibody functions helped develop modern vaccines. In addition, surface proteins of B cells are currently being researched for their potential as immune checkpoints in cancer immunotherapy. Meanwhile, T cells are used in cancer treatment to recognize and kill cancer cells by genetically modifying them with chimeric antigen receptors (CAR T-cell therapy). [16,17]

## 2. G-protein-coupled receptors (GPCRs)

G-protein coupled receptors are seven-transmembrane-domain proteins responsible for a variety of intracellular signaling pathways, instigated by extracellular stimuli. Their relevance is reflected by their involvement in a wide range of physiological responses and diseases, making them suitable drug targets for therapeutic intervention. On the cytosolic

side the heterotrimeric guanine protein (G-protein), consisting of an α, β and γ subunit, is linked to the receptor. G-protein subclasses ($G_s$, $G_{i/o}$, $G_{q/11}$ and $G_{12/13}$) are differentiated by their interaction with a variety of intracellular effectors resulting in different cellular responses. For instance, $G_s$ and $G_{i/o}$ both regulate adenylyl cyclase (AC) activity. [1–3,13]

The $G_\alpha$ subunit is linked to GDP (guanosine diphosphate), which ensures the protein complex stays associated. After the activation of the receptor through extracellular stimuli, a G-protein-dependent (classical way) or -independent signaling pathway is triggered. The conformational changes of the GPCR, instigated by ligand binding lead to the dissociation of the $G_\alpha$ subunit form the $G_{\beta\gamma}$ complex and the replacement of GDP by GTP (guanosine triphosphate). Since the intracellular GTP concentration is high, it can quickly dock onto the $G_\alpha$ subunit. Both subunits influence the signaling pathway differently after being separated. The alpha subunit interacts with effector proteins like adenylyl cyclase (AC) and phospholipase C (PLC). While the βγ-complex regulates phospholipase Cβ (PLCβ), phosphoinositide 3-kinase (PI3K) and ion channels. To terminate the GPCR signaling pathway, GTP is hydrolyzed to GDP initiating the reassociation of the subunits to the heterotrimeric G-protein. [1–3,13]

One of the more relevant intracellular mediators of GPCR is adenylyl cyclase, which is activated by the stimulatory $G_\alpha$ subunit and inhibited by $G_{i/o}$. After its activation, it converts ATP into cyclic adenosine monophosphate (cAMP) increasing its intracellular concentration. Cyclic adenosine monophosphate is an essential mediator for multiple signaling pathways and regulates a wide range of cellular responses through its effectors such as Protein kinase A (PKA) and exchange proteins directly activated by cAMP (EPAC). PKA is an essential cAMP-regulated effector responsible for many of the downstream functions. Due to the involvement of the second messenger cAMP in multiple signaling pathways concerning the regulation of inflammation, metabolism and other functions it has been viewed as an attractive target for therapeutic intervention. [2,18]

The focus of this study was on the influence of GPCR's on innate immunity. To be more precise, the regulation of anti- and pro-inflammatory responses through GPCR signaling pathways. While it is well-known that macrophages and neutrophils are commonly activated by invading pathogens or cytokines, their activity can also be mediated through

GPCR's. Therefore, this study researched two receptors, TGR5 and GPR84, which are expressed on these immune cells. [19–21]

## 2.1 Takeda G-protein coupled receptor 5 (TGR5)

TGR5 or Takeda G-protein coupled receptor 5 or G-protein coupled bile acid receptor 1 (GPBAR 1) is a GPCR expressed in a range of cell types such as epithelial cells of the intestines or in the gallbladder. But TGR5 is also highly expressed in Kupffer cells and macrophages. Due to TGR5 expression in different tissues and organs, its functions vary depending on where it is found. For instance, in the liver, it protects against hepatosteatosis, in the gallbladder it mediates relaxation of smooth muscles and on macrophages it induces anti-inflammatory responses. Therefore, gaining interest as a potential target for treating inflammatory disease. [5,22,23]

Its activity is regulated by secondary bile acids (lithocholic acid and taurolithocholic acid), microbial byproducts of primary bile acids, which were synthesized from the cholesterol metabolism. These secondary bile acids circulate in the enterohepatic tract and induce the resorption of dietary lipids, but can also function as signal molecules, in this case as endogenous ligands for TGR5. After the stimulation of TGR5 through endogenous ligands, for example lithocholic acid (LCA), it undergoes a conformational change resulting in the dissociation of the stimulatory $G_{\alpha}$ subunit coupled with GTP. Subsequently, the subunit activates AC to increase intracellular cAMP levels (**Figure 2**). The second messenger initiates signal transduction by binding to PKA, which then phosphorylates cAMP response element-binding protein (CREB) and protein kinase B (AKT). This results in the release of Glucagon-like peptide-1 (GLP-1). In addition, increased intracellular $Ca^{2+}$ concentration induced by PKA leads to enhanced GLP-1 secretion. GLP-1 heightens insulin sensitivity and promotes energy metabolism causing weight loss. [5,22,24–26]

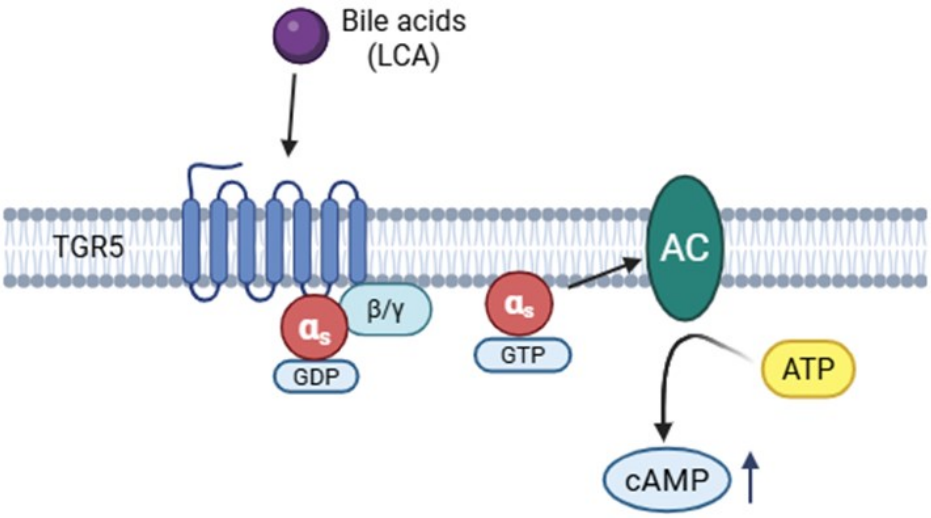


**Figure 2**. *Schematic overview of the TGR5 signaling pathway.*

The binding of bile acids to TGR5 leads to a conformational change in the receptor through which the dissociation of the alpha subunit from the G-protein complex is induced. This subunit then activates adenylyl cyclase (AC) to start converting ATP to cAMP. The second messenger cAMP induces a variety of cell responses through its downstream effectors. [25]
**AC** = Adenylyl cyclase, **ATP** = Adenosine triphosphate, **cAMP** = Cyclic adenosine monophosphate, **GDP** = Guanosine diphosphate, **GTP** = Guanosine triphosphate, **LCA** = Lithocholic acid, **TGR5** = Takeda G-protein coupled receptor 5; Created with Biorender.com

Other biological effects caused by TGR5 activation are of anti-inflammatory nature. Phosphorylated CREB mediates the repression of pro-inflammatory transcription factor nuclear factor kappa-B (NF-κB) through two different mechanisms. Firstly, it activates effector mammalian target of rapamycin (mTOR), which increases concentrations of liver inhibitory protein (LIP). This protein binds onto DNA and therefore inhibits the expression of many pro-inflammatory genes including NF-κB-dependent genes. This signaling pathway is also stimulated through AKT. Secondly, CREB achieves inhibitory effects by activating signal transducer and activator of transcription 1 (STAT1). The STAT1-mediated signaling pathway leads to inhibition of NF-κB thus reducing the expression of pro-inflammatory cytokines, such as Interleukin-1β (IL-1β), IL-6 and tumor necrosis factor α (TNFα). [21,22]

Another pro-inflammatory effector affected by TGR5 signaling is inflammasome NLRP3 (NOD-like receptor protein). Activation of this inflammasome results in the release of pro-inflammatory cytokines like IL-1β and IL-18. Subsequently, progression of inflammatory diseases such as type 2 diabetes, atherosclerosis, gout and many more is induced. Its assembly can be prevented by the cAMP-PKA pathway initiated through TGR5 activation.

As a result, the release of cytokines is inhibited, therefore reducing inflammatory reactions. [22,27]

Due to its involvement in several anti-inflammatory signaling pathways, TGR5 has been recognized as a potential therapeutic target. Many *in vitro* and *in vivo* studies have been conducted to evaluate the therapeutic relevance of this GPCR in various inflammatory diseases. For instance, its role in atherosclerosis has been studied in mouse models. In mice it was observed that TGR5 inhibited inflammation in macrophages and decreased their LDL uptake. This resulted in the inhibition of atherosclerosis development induced by a high cholesterol diet. These findings further support the relevance of researching TGR5 for its therapeutic potential. [28]

## 2.2 G-protein coupled receptor 84 (GPR84)

The orphan G-protein coupled receptor 84 (GPR84) has been identified as a medium-chain fatty acid (MCFA) receptor. Although the knowledge about this GPCR is lacking, it is known that GPR84 is expressed, though limited, in epithelial cells of the esophagus, large intestines, adipocytes and leukocytes. Specifically, neutrophils and macrophages show high expression rates of this receptor. Various studies have observed that GPR84 expression can be increased by inflammatory conditions or a high medium-chain fatty acids diet. A study conducted in rats and findings collected from human endoscopic biopsies described high expression levels because of inflammation induced by reflux esophagitis. Even dietary MCFAs, the proposed endogenous ligands of GPR84, could elevate the expression levels. These findings suggest GPR84 as a possible therapeutic target for inflammatory diseases such as reflux esophagitis, osteoarthritis, ulcerative colitis and many more. [4,29–32]

Upon activation of GPR84 through MCFAs the dissociation of the heterotrimeric G-protein, from the $G_{i/o}$ subclass, is initiated. The inhibitory $G_{\alpha}$ subunit blocks AC from converting ATP into cAMP, reducing the intracellular cAMP levels (**Figure 3**). [32–34]

This signaling pathway induces the expression and secretion of pro-inflammatory cytokine TNFα, IL-6 and IL-1β. In addition, GPR84 mediates neutrophil migration. [20,33]

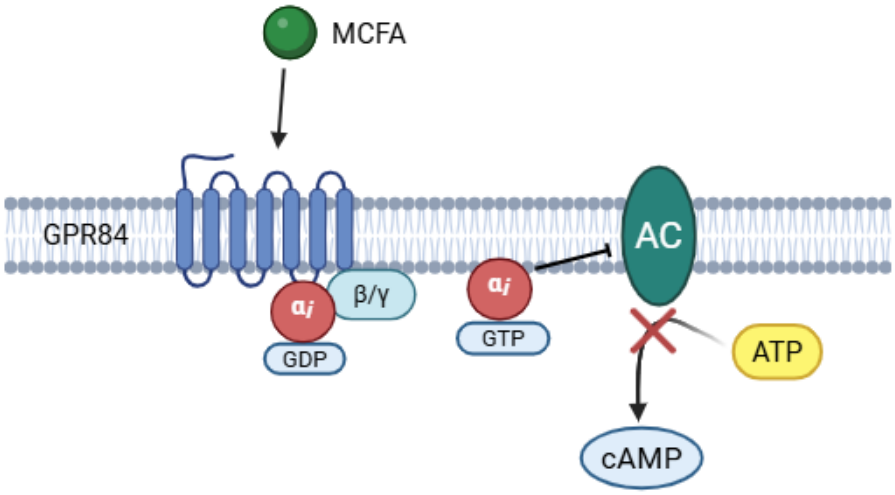


**Figure 3.** *Schematic overview of the GPR84 signaling pathway.*

When the GPR84 receptor is activated by the binding of MCFAs a signaling pathway mediated by the inhibitory G-protein is mediated. The alpha subunit, linked with GTP, inhibits AC and stops the process of converting ATP into second messenger cAMP.
**AC** = Adenylyl cyclase, **ATP** = Adenosine triphosphate, **cAMP** = Cyclic adenosine monophosphate, **GPD** = Guanosine diphosphate, **GPR84** = G-protein coupled receptor 84, **GTP** =Guanosine triphosphate, **MCFA** = Medium-chain fatty acid; Created with BioRender.com

Due to the knowledge that neutrophil migration can be GPR84-mediated, several studies have focused on investigating their interaction and possible clinical benefits. One study highlighted how the migration of neutrophils into inflamed colonic tissue was reduced by using GLPG1205, a known GPR84 antagonist. They induced chronic inflammatory bowel disease in mice using dextran sodium sulfate (DSS). [4] Another study conducted experiments in mice with acute lung injury (ALI) induced via lipopolysaccharide (LPS) injections. They concluded that by inhibiting GPR84 with small molecules or decreasing its expression caused a reduction of migrated neutrophils into the lungs. This was determined through the analysis of cells in bronchoalveolar lavage fluid (BALF). [20]

While current knowledge of GPR84 is limited, its role in inflammation is becoming increasingly evident. This suggests more research should be conducted to not only evaluate its potential as a target for anti-inflammatory drug development but also deepen the understanding of its involvement in physiological and pathological aspects. [35]

## B. Aim of this study

The aim of this study was to identify potential compounds from the DNTI (Drugs from nature targeting inflammation, a FWF-funded research network from 2008 to 2014) project that influence the cAMP signaling pathway. The second messenger cAMP plays an important role in cellular signaling pathways due to its involvement in multiple pathways concerning regulation of inflammation, metabolism and other functions. [18] Therefore, the receptors TGR5 and GPR84 were selected, due to their relevance to cAMP signaling and influence on macrophages and neutrophils, components of the innate immunity.

Due to the anti-inflammatory nature of TGR5, the therapeutic focus was on identifying compounds with agonistic properties. To assess the ligand-receptor interaction, a target-based screening investigating cAMP/CRE signaling pathway was applied. This seemed appropriate, as TGR5 activation leads to elevated intracellular cAMP levels and thereby triggers anti-inflammatory responses. A stable cell line expressing the TGR5 receptor was used for the screening process. Additionally, to determine target-specificity the compounds were simultaneously tested in a non-TGR5 expressing control cell line.

Meanwhile, the pro-inflammatory nature of GPR84 set the therapeutic focus on identifying compounds with antagonistic properties. Ligand-receptor interaction was assessed with an EPAC-based fluorescence resonance energy transfer (FRET) biosensor to quantify intracellular cAMP concentrations. [36] This was deemed appropriate, as GPR84 activation leads to a reduction of intracellular cAMP levels and the opposite effect was achieved with antagonists. Once potential candidates were identified, further testing was conducted to analyze their antagonistic behavior and their effect on neutrophil migration.

# C. Material and Methods

## 1. Compounds

The screening for potential TGR5 agonists and GPR84 antagonists was carried out with compounds from the "Drugs from nature targeting inflammation (DNTI)" project. The DNTI databank was a national research project developed from six Austrian universities with the objective of identifying and characterizing anti-inflammatory natural products (NP). Apart from plant extracts isolated pure substances, semi-synthetic and synthetic compounds are also included. Compounds not included in this project will be mentioned separately. This included the microbial flavonoid metabolites, listed in the appendix, which were available undissolved and had to be prepared as 30 µM solutions using DMSO 0.1% as the solvent. [37,38]

## 2. Cell culture

To prevent microbial contamination human embryonic kidney cells 293 (HEK293) and human lung adenocarcinoma cells (Calu-3) were handled under a laminar air flow workbench (HERAsafe®KS18). By sanitizing the surface of the laminar hood with Hexaquart plus 1% (B. Braun, Melsungen, Germany) and ethanol (EtOH) 70%, before beginning the working process, further risks of possible contamination could be reduced.

For a steady growth rate and good cell viability, HEK293 cells were passaged every other day, whereas Calu-3 cells only once a week, depending on their confluence, however a media change was performed every other day. The cell cultures were maintained in the HERAcell® 150 incubator at 37°C and 5% $CO_2$. HEK293 cells were cultured in complete medium (CM) and Calu-3 cells in Dulbecco's Modified Eagle Medium/Nutrient Mixture F-12 (DMEM/F-12), both in 175 $cm^2$ culture flask (T-175 Sarstedt, Germany). To ensure no damage was caused towards the cells, all needed liquids were prewarmed for approximately 30 minutes in the water bath Julabo® SW23 at 37 °C.

All materials used in cell culture are listed in **Table 1**.

*Table 1. Used liquids in cell culture.*

| Material | Ingredients | Amount | Source |
|---|---|---|---|
| **Complete Medium (CM)** | DMEM with phenol red | 500 ml | Sigma-Aldrich (Vienna, Austria) |
| | 4,5 g/l glucose | | Gibco (Lofer, Austria) |
| | FBS | 50 ml | Lonza (Basel, Switzerland) |
| | L-Glutamine (2 mM) | 5 ml | Lonza (Basel, Switzerland) |
| | Penicillin (100 U/ml) | 5 ml | |
| | Streptomycin (100 µg/ml) | | |
| **DMEM/ F-12** | DMEM with phenol red | 500 ml | Sigma-Aldrich (Vienna, Austria) |
| | 4,5 g/l glucose | | Sigma-Aldrich (Vienna, Austria) |
| | Ham's F-12 Nutrient Mix | 500 ml | Gibco (Lofer, Austria) |
| | | | Lonza (Basel, Switzerland) |
| | FBS | 2 x 50 ml | Lonza (Basel, Switzerland) |
| | L-Glutamine (2 mM) | 2 x 5 ml | |
| | Penicillin (100 U/ml) | 2 x 5 ml | |
| | Streptomycin (100 µg/ml) | | |
| **Stripped Medium** | DMEM with phenol red | 500 ml | Sigma-Aldrich (Vienna, Austria) |
| | 4,5 g/l glucose | | Gibco (Lofer, Austria) |
| | Charcoal stripped FBS | 25 ml (5%) | Lonza (Basel, Switzerland) |
| | L-Glutamine (2 mM) | 5 ml | Lonza (Basel, Switzerland) |
| | Penicillin (100 U/ml) | 5 ml | |
| | Streptomycin (100 µg/ml) | | |
| **PBS** | $ddH_2O$ | 100 ml | |
| | NaCl | 7,2 g | Carl-Roth (Karlsruhe, Germany) |
| | $Na_2HPO_4$ | 1,48 g | Carl-Roth (Karlsruhe, Germany) |
| | $KH_2PO_4$ | 0,43 g | Carl-Roth (Karlsruhe, Germany) |
| **Trypsin/ EDTA** | Trypsin | 0,5 g | Gibco (Lofer, Austria) |
| | EDTA | 0,2 g | Carl-Roth (Karlsruhe, Germany) |
| | PBS | ad 1000 ml | |

## 2.1 Cell lines

### 2.1.1 Modified HEK293 cell lines

Mainly these following stable cell lines were used for experiments in this thesis:

- TGR5 EPAC HEK293
- EPAC HEK293
- GPR84 EPAC HEK293.

These are genetically modified stable HEK293 cell lines, derived from the human embryonic kidney cells. All cell lines were stably transfected with a gene encoding EPAC. One cell line was further modified to express the GPCR TGR5 and another to express GPR84, both not commonly expressed in HEK293 cells. The EPAC HEK293 cells were void of both GPCRs and were therefore used as the control cell line. They show adherent growth behavior, rapid proliferation and adaptability to various experimental conditions. Thus, making them well-suited for transfection and receptor stimulation studies. [39,40]

As mentioned before, to maintain steady growth rate and good cell viability they were passaged on a regular basis whenever they reached ~80% confluence. Before subculturing all necessary liquids were prewarmed to not harm the cells due to cold temperatures. While the substances were warmed up in the water bath Julabo® SW23 at 37 °C the laminar workbench HERAsafe®KS18 was sterilized with Hexaquart plus 1% (B. Braun, Melsungen, Germany) and ethanol 70%. This was done every time before and after working under the laminar workbench HERAsafe®KS18. To minimize the risk of contamination , the complete medium (CM), PBS, trypsin and anything else put under the hood were sprayed with EtOH 70%. After preparing everything, the cells were put lastly under the hood, thus the process of passaging the cells could start. Firstly, the old medium was removed, and 10 ml of PBS was added to wash away remnants of CM and dead cells. Having discarded the PBS, 4 ml of trypsin was pipetted into the culture flask (T-175 Sarstedt, Germany) to detach the cells from the flask surface. It is important that the trypsinization was not prolonged, as it may lead to cell surface proteins being degraded resulting in lower cell viability. [41] Therefore, the incubation time should not be longer than 5 minutes. To neutralize trypsin, 8 ml of CM was dispersed on the flask surface by repeatedly pipetting the media up and down. The cell suspension was then transferred into a 50 ml falcon tube (Sarstedt, Germany) and put into the centrifuge (Heraeus™ 1 S-R

Multifuge, Germany) for 4 minutes at 1400 g. Afterwards the supernatant was discarded, and the obtained cell pellet resuspended in 11 ml CM. To determine the number of cells in the suspension 1 ml was filled into a vial for the Vi-Cell™ XR cell viability Analyzer (Beckman Coulter, USA). For subculturing, 8 x $10^6$ cells were seeded into a culture flask (T-175 Sarstedt, Germany), so the required volume of cell suspension was calculated and adjusted to a final volume of 20 ml with CM. After finishing the passage, HEK293 cells were put back into the HERAcell® 150 incubator at 37°C and 5% $CO_2$. [38]

### 2.1.2 Calu-3 cell line

Calu-3 cells are human airway epithelial cells originally isolated from lung adenocarcinoma. They exhibit key features such as tight junction, desmosomes and microvilli making them well-suited for simulating epithelial layers. Their ability to form polarized monolayers with tight junctions makes them valuable for experiments with needed barrier integrity. Therefore, Calu-3 cells were suitable for studies investigating cellular response to induced injury, drug transport and functional barrier characteristics. [42,43]

Since Calu-3 cells proliferated at a slower pace than HEK293 cells, they were passed once a week, if they reached approximately 80% confluence. This was visually checked under the Olympus CKX31 microscope. However, the culture medium was changed on alternate days. The subculturing process is similar to HEK293 cells, with a few adjustments as follows.

To begin, the workbench HERAsafe®KS18 was cleaned with Hexaquart plus 1% (B. Braun, Melsungen, Germany) and 70% ethanol. Pre-warmed PBS, trypsin and DMEM/F12, were put under the hood. Firstly, the old media was removed, and 10 ml of PBS was added to wash away remnants of dead cells and media residues. This was followed by replacing PBS with 7 ml trypsin. A higher volume was needed for Calu-3 cells since they do not detach easily. After letting them incubate for approximately 15 minutes, 14 ml of DMEM/F12 was used to neutralize trypsinization. The resulting cell suspension was filled into a 50 ml falcon tube (Sarstedt, Germany) and put into the centrifuge (Heraeus™ 1 S-R Multifuge, Germany) for 4 minutes at 1400g. Afterwards, the supernatant was discarded, and the remaining cell pellet was resuspended in 11 ml DMEM/F12. To determine the number of Calu-3 cells, 1 ml of suspension was used to for the Vi-Cell™ XR cell viability

Analyzer (Beckman Coulter). For subculturing, 5 x $10^6$ cells were seeded into a culture flask (T-175 Sarstedt, Germany), and the required volume of cell suspension was calculated and adjusted to a final volume of 20 ml with DMEM/F12. Once the passaging was completed, Calu-3 cells were put back into the HERAcell® 150 incubator at 37 °C and 5% $CO_2$.

## 3. CRE-Luciferase Assay

To identify potential agonists for the anti-inflammatory G-protein coupled receptor TGR5, a CRE-luciferase assay was performed. To assess the specificity of those compounds towards the receptor they were simultaneously tested in non-TGR5-expressing EPAC-HEK cells. Compounds showing an increase of intracellular cAMP levels in EPAC cells, independent from TGR5, were deemed unspecific since the elevation was achieved through alternative signaling pathways.

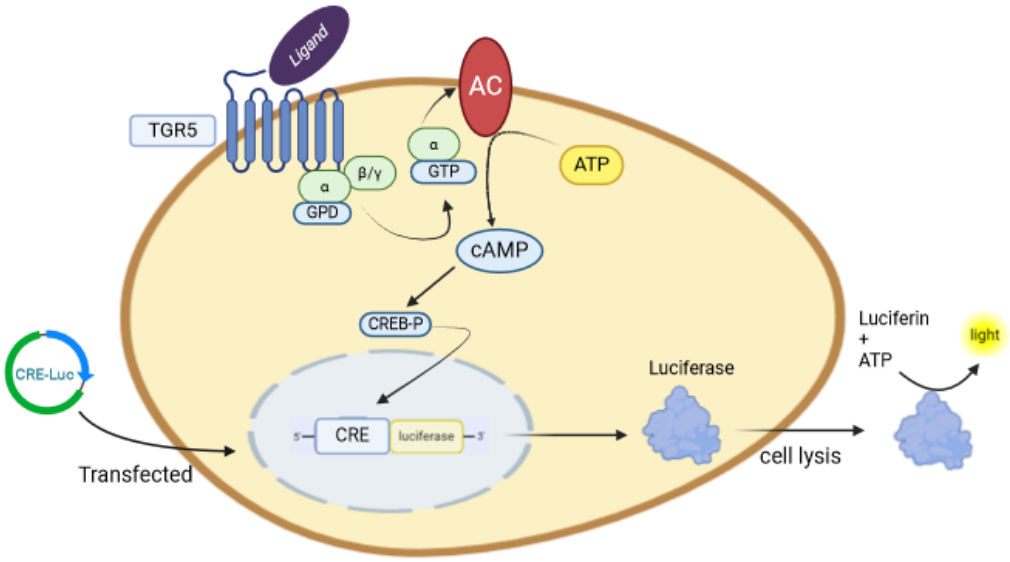


**Figure 4.** *Schematic overview of the CRE-Luciferase assay.*

The first step was the seeding of cells and transfection. This was followed by compound treatment. As seen in the figure, the binding of the ligand to the receptor leads to the release of the alpha subunit, which activates adenylyl cyclase. Under the use of ATP intracellular cAMP levels were increased. Through the activation of CREB-P (cAMP responsive element binding protein) luciferase was expressed. Via cell lysis luciferase was released and quantified by adding ATP and luciferin, resulting in the emission of light.
**ATP** = Adenosine triphosphate, **cAMP** = Cyclic adenosine monophosphate, **CRE** = cAMP responsive element, **TGR5** = Takeda G-protein receptor 5; Created by BioRender.com

The assay is divided into three parts, which span over three days: Seeding and transfection, compound treatment and lastly measurement. A schematic overview of the CRE-Luciferase assay is shown in **Figure 4**.

To begin, TGR5 EPAC HEK293 cells were passaged on the first day by seeding 8 x $10^6$ cells into a 150 mm petri dish (Sarstedt, Germany) for the luciferase assay while also seeding them into a culture flask for further subculturing. Simultaneously EPAC HEK293 cells were prepared in the same way. Then the dishes were incubated at 37 °C and 5% $CO_2$ for 5 to 6 hours. For the transfection a mixture of CRE-Luc (cAMP response element - luciferase) reporter plasmid, HEPES-buffered-saline (2x HBS), 2 M $CaCl_2$ and $ddH_2O$ were mixed (**Table 2**). Firstly, $ddH_2O$, 2x HBS and CRE-Luc plasmid were mixed into an Eppendorf tube and vortexed (VM-3000 Mini Vortexer) very thoroughly. Lastly, $CaCl_2$ was added to the solution. Ater having vortexed the mixture again it was left under the workbench for 20 minutes to incubate before being pipetted onto the dishes. [38]

*Table 2.Ingredients for transfection solution*.

| Material | Ingredients | Amount | Source |
|---|---|---|---|
| **Transfection mix** | CRE-Luc | 10 µg | Promega (Madison, Wi, USA) |
| | 2 X HBS | 750 µl | |
| | $CaCl_2$ (2 M) | 94 µl | Sigma-Aldrich (Vienna, Austria) |
| | $ddH_2O$ | ad 1500 µl | |

While the composition incubates, the TGR5 and EPAC cells are visually checked under the Olympus CKX31 microscope with 10x and 20x magnification to ensure they have adhered to the surface of the petri dish, as seen in **Figure 5A**. Once the incubation time was completed, the cells were immediately transfected. This was followed by an overnight incubation at 37 °C and 5% $CO_2$.

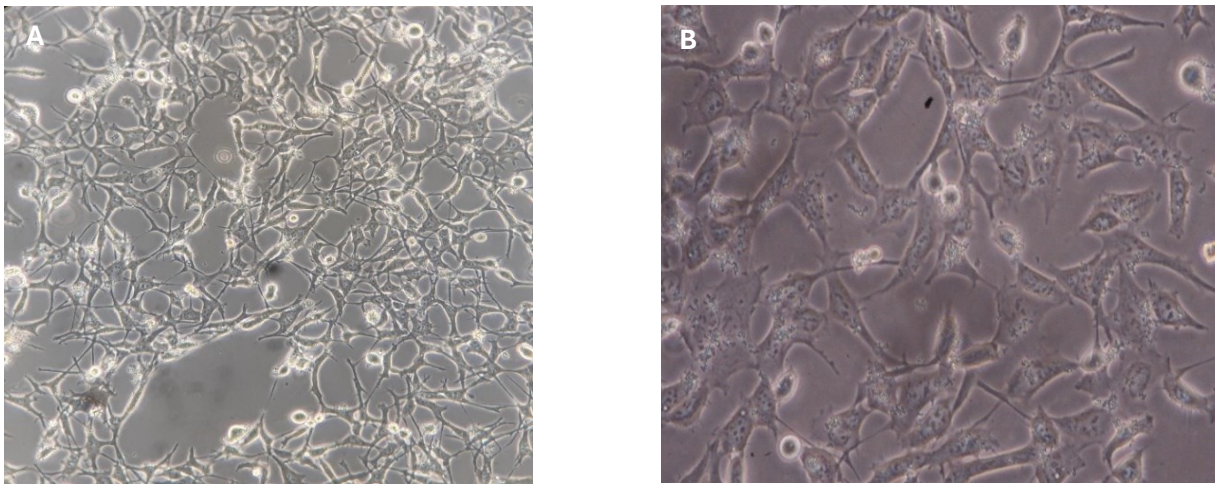


**Figure 5**. *TGR5-HEK cells before transfection in 10x magnification (A) and after transfection and overnight incubation (B) in 20x magnification*.
Pictures taken by author

The second part of the luciferase assay was compound treatment. First, the overnight transfected cells were visually inspected (**Figure 5B**), then underwent a media change with fresh CM and were put back into the HERAcell® 150 incubator for at least 4 hours. While the cells were resting, preparations for the compound treatment were made. To begin with, the substances were diluted 1:250 in prewarmed stripped medium (SM). Once these dilutions were completed, they were vortexed (VM-3000 Mini Vortexer) and pipetted onto Cellstar® 96 well plates. Four wells in a column were loaded with 50 µl of a compound dilution each. The first two columns contained the negative control DMSO 0.1% and the positive control lithocholic acid (LCA) 10 µM. The layout of the Cellstar® 96-well plate is shown in **Figure 6,** with "– " indicating DMSO 0.1% and "+" representing LCA 10 µM. Everything between LCA 10 µM and background was filled with compounds. Once both plates were prepared, they were incubated until the cells were ready to be transferred onto them. [38]

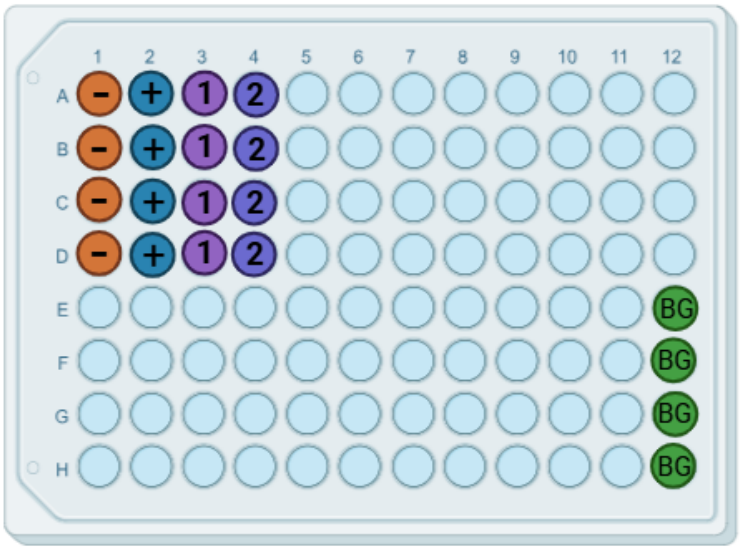


**Figure 6**. *Layout of a 96-well plate for luciferase assay.*

Wells labeled "- "contained DMSO 0.1% (negative control) while "+" contained the positive control lithocholic acid (10 µM). Labels "1" and "2" represent different compounds whereas "BG" (background) was left empty. Created with BioRender.com

For the splitting of cells CM, PBS, SM and trypsin were required. Firstly, the old medium was removed, and 10 ml of PBS was added to wash away remnants of CM and dead cells. Having discarded, PBS 4 ml of trypsin was pipetted into the petri dish. After letting them sit for 5 minutes, CM was used to neutralize trypsin and the cell suspension was then filled into a 50 ml falcon tube (Sarstedt, Germany) followed by a centrifuge cycle (Heraeus™ 1 S-R Multifuge, Germany) for 4 minutes at 1400g. Afterwards, the supernatant

was discarded, and the obtained cell pellet resuspended in 11 ml SM. To determine the cell concentration 1 ml of suspension was used in the Vi-Cell™ XR cell viability Analyzer (Beckman Coulter). For a 96-well plate a cell density of 0,33 x $10^6$ per ml was needed. So, the cell suspension was diluted with SM until that concentration was reached. Subsequently, each well was filled with 150 µl of the suspension except for the last four wells. Once both plates, one for TGR5 and the other for EPAC, were arranged they were put in the HERAcell® 150 incubator at 37 °C and 5% $CO_2$ for 18 hours. [38]

The last part of the assay was the measurement. After 18 hours of incubation, the plates were taken out of the incubator and visually checked under the Olympus CKX31 microscope. This was necessary to determine whether compounds showed signs of cytotoxicity, as there would be dead cells visible in the wells. Afterwards, the supernatant above the cells was removed by vacuum and the plates were frozen at -70 °C for one hour. Meanwhile, a lysis buffer was prepared. The ingredients are listed in **Table 3**. Each well was loaded with 50 µl of this liquid after which the plate was transferred onto the Multi-Microplate Genie™ Shaker for 10 minutes. This was then followed by pipetting 40 µl of the suspension into a new black 96-well plate and ensuring the surface was fully covered with the liquid. The measurement was achieved with the TECAN Spark® Microplate Reader, through which fluorescence and luminescence were measured. [38]

The luminescence was determined by using the injector on the TECAN Spark® Microplate Reader to inject each well with an ATP and luciferin solution. When the enzyme luciferase binds to luciferin in the presence of ATP, it leads to the oxidation of luciferin which is followed by the emission of light. Therefore, the intensity of the light and the amount of luciferase activity can be put into direct relation. [44–46]

## 3.1 Statistical Analysis

The results gathered through the TECAN Spark® Microplate Reader were then used to determine the mean values for the technical quadruplicates with Microsoft office excel. Before the ratio between relative luminescence (RLU) and relative fluorescence (RFU) was calculated, the mean values of the background wells were subtracted. This ensured that the recorded signals were solely from the cells. Next, the ratios were normalized to the vehicle DMSO 0.1%, which stood for the baseline value. Three independent biological experiments were conducted to assess the statistical significance of the results (p-value

< 0.05). Statistical analyses were completed by a One-way-ANOVA test on GraphPad Prism 6.01. [38]

*Table 3. Substances used during measurement.*

| Material | Ingredients | Amount (For one 96-well plate) | Source |
|---|---|---|---|
| **Lysis Buffer** | Lysis Buffer 5X | 4,8 ml | Promega (Wi, USA) |
| | $ddH_2O$ | 1,2 ml | |
| | Coenzyme A (CoA) | 2 µl | Sigma- Aldrich (Vienna, Austria) |
| | DTT (Dithiothreitol) | 6 µl | Fluka (Vienna, Austria) |

## 4. EPAC FRET Biosensor

Since cAMP is responsible for the regulation for a variety of cellular signaling, different strategies were developed over time to visually quantify cAMP levels in living cells. One of these being the EPAC FRET biosensor. FRET, short for Förster Resonance Energy Transfer, is a biophysical phenomenon used to learn about molecular interaction at close distance. The sensor is composed of three parts: a cAMP-binding domain EPAC (Exchange protein directly activated by cAMP), a donor fluorophore CFP (cyan fluorescence protein) and an acceptor fluorophore Venus. The fluorophores are fused with EPAC in proximity allowing energy transfer. If the intracellular cAMP levels remain low, then no interaction occurs between EPAC and cAMP leading to FRET. Therefore, fluorescence is primarily emitted at 520 nm (Venus) when excited at 420 nm. However, when cAMP binds onto EPAC a conformational change occurs, resulting in a disruption of energy transfer because of the increased distance. As a result, fluorescence is emitted at 480 nm (CFP), while the acceptor (Venus) fluorescence is decreased (**Figure 7**). [18,26,34,47]

This approach allowed not only the direct determination of cAMP concentrations but also studied the role of GPCR modulating cAMP levels in response to external stimuli. Since GPR84 antagonists are expected to result in an elevation of intracellular cAMP levels, the use of EPAC FRET biosensor was an effective method to investigate these changes in real time. [18]

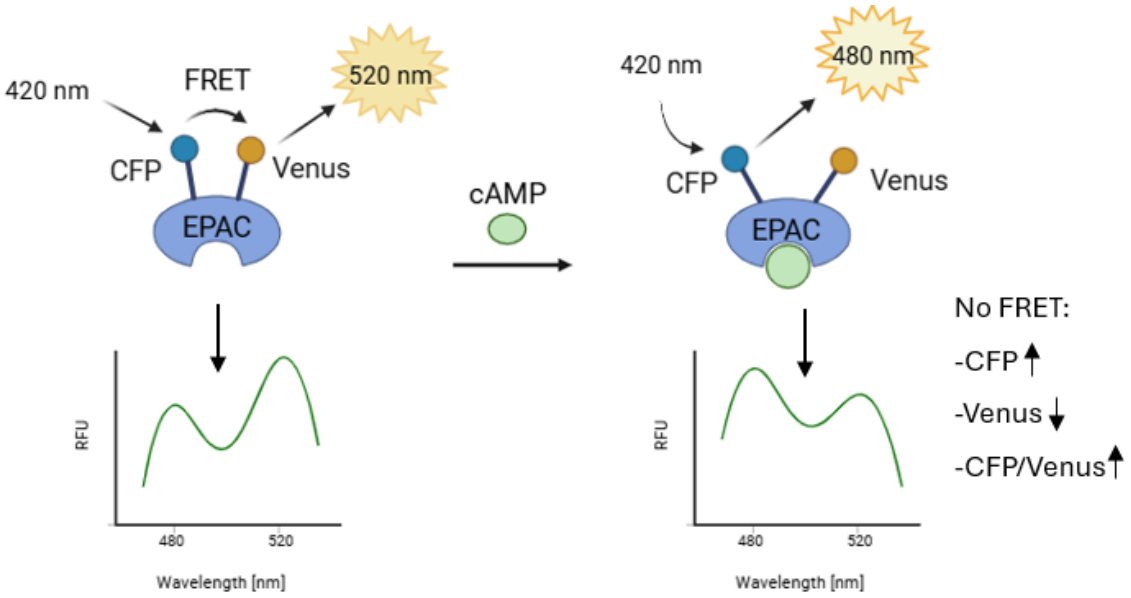


**Figure 7.** Mechanism of the EPAC FRET biosensor.

In the absence of cAMP, acceptor and donor fluorophore stay in proximity, allowing energy transfer (FRET). This results in fluorescence emission at 520 nm. If the intracellular cAMP levels are increased, it binds to EPAC and separates CFP and Venus from each other via conformational change, therefore disrupting FRET. In this case, less energy is transferred to the acceptor fluorophore, and the emission is seen at 480 nm. [34] **cAMP** = Cyclic adenosine monophosphate, **CFP** = cyan fluorescence protein, **EPAC** = exchange protein directly activated by cAMP, **FRET** = Förster Resonance Energy Transfer, **RFU** = relative fluorescence unit Created with BioRender.com

## 4.1 EPAC Assay

To screen for potential antagonist for the pro-inflammatory receptor GPR84 the EPAC assay was used. To verify if those compounds were specific for the G-protein coupled receptor (GPCR) they were simultaneously tested on EPAC-HEK cells. Once an effect was visible in EPAC cells without the GPR84 receptor, these substances were deemed unspecific.

The assay was divided into two parts, which spanned over two days: seeding of the cells and compound treatment followed by measurement. A schematic overview can be seen in **Figure 8**. To begin with, GPR84 EPAC HEK293 cells were passaged on the first day by seeding 200 µl with a cell number of 0,15 x $10^6$ cells per well into the upper half of the Cellstar® 96-well plate while the rest of the cell suspension was used to seed cells into a culture flask (T-175 Sarstedt, Germany) for further subculturing. Simultaneously EPAC HEK293 cells were prepared the same way but seeded into the lower half of the plate. The layout of the plate can be seen in **Figure 9.** Then the cells were incubated at 37 °C and 5% $CO_2$ overnight. [38]

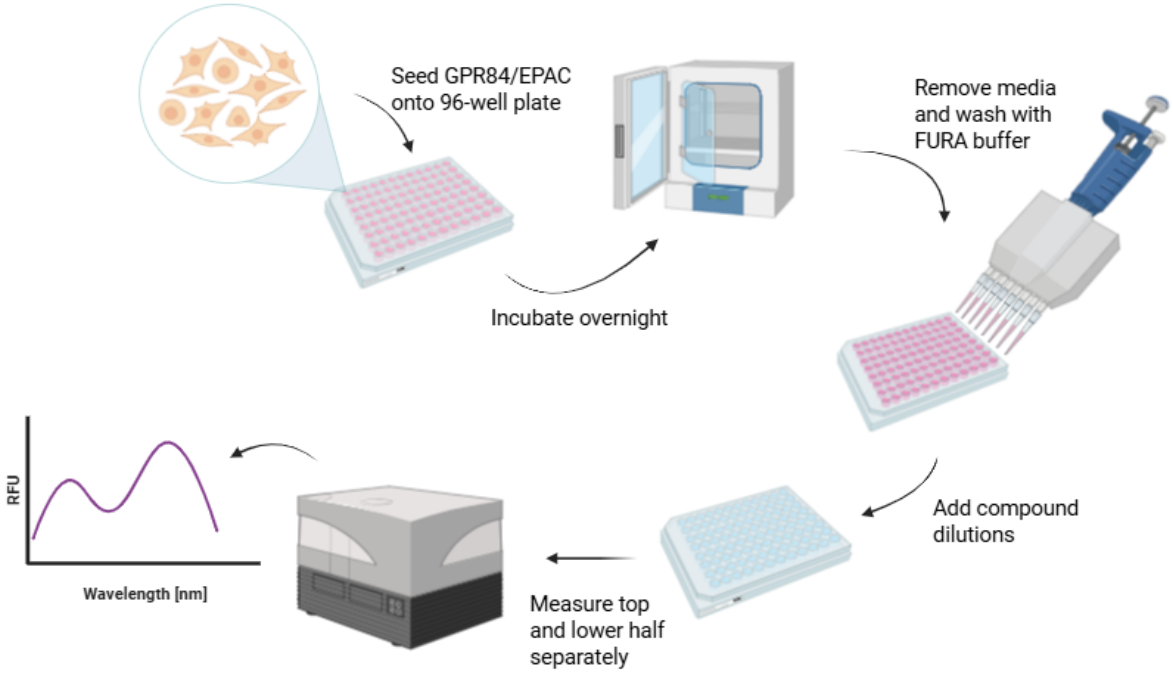


**Figure 8.** *Schematic overview of EPAC assay.*

At the beginning GPR84 and EPAC cells were seeded onto a 96-well plate. The cells were incubated overnight and taken out the next day to remove the media and wash them with FURA buffer. After adding the compound dilutions, the plate was put into the TECAN. Both halves were measured separately to obtain biological triplicates for each cell line. **EPAC** = Exchange Protein directly activated by cAMP, **GPR84** = G-protein coupled receptor 84, **RFU** = Relative fluorescence unit; Created with BioRender.com

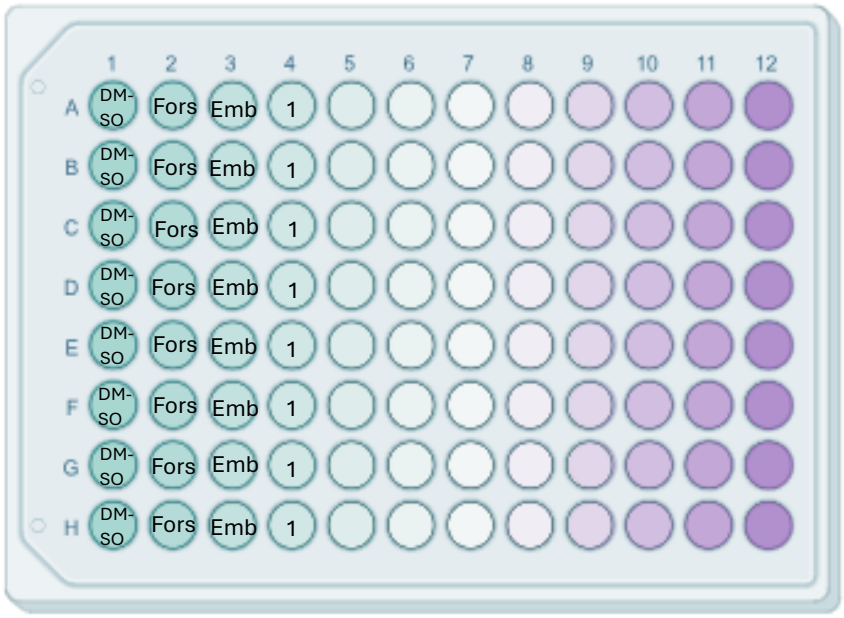


**Figure 9.** *Layout of a 96-well plate in EPAC assay.*

GPR84 HEK-EPAC cells were seeded in rows A-C and EPAC cells in E-G of the 96-well plate. Rows D and H remained empty for the background signal. Each column was filled with different compounds. The first three contained controls DMSO 0.1%, Forskolin and Embelin. The columns onward were loaded with compounds.
**DMSO** = Dimethyl sulfoxide; **Fors** = Forskolin; **Emb** = Embelin + Forskolin; Created with BioRender.com

On the next day, the tested substances were prepared for compound treatment. Since the aim of this assay was to screen for potential antagonists, the compounds were co-treated with the controls Forskolin and Embelin. Forskolin is an activator for adenylyl cyclase, therefore leading to increased intracellular cAMP levels whereas Embelin, a GPR84 agonist, causes the opposite effect. [48,49] The preparation for the compounds was as follows: first the controls were prepared. Three Eppendorf tubes were filled with 997 µl FURA buffer. In the first tube 3 µl DMSO were added, this being the negative control. In the second tube 2 µl DMSO and 1 µl Forskolin (10 µM) were pipetted. In the third tube 1 µl DMSO, 1 µl Embelin (1 µM) and 1 µl Forskolin (10 µM) were added. Afterwards, the co-treatment mixture for the compounds was completed by mixing 30 ml FURA buffer (**Table 4**) with 30 µl Forskolin (10 µM) and 30 µl Embelin (1 µM) in a 50 ml falcon tube (Sarstedt; Germany). The tube was vortexed before pipetting 999 µl into each Eppendorf tube. Subsequently, 1 µl of the compounds were added to the tubes. Since one column represented one compound, nine substances could be measured simultaneously. The solutions were vortexed (VM-3000 Mini Vortexer) and pipetted into a clear Cellstar® 96-well plate with a volume of 125 µl/well. Once that plate was arranged, the overnight incubated cells were visually inspected with the Olympus CKX31 microscope. Next, the medium on the top of the adherent cells was carefully removed and followed by a washing step with 150 µl/well FURA buffer. Lastly, the buffer was discarded and replaced with 100 µl/well compound dilution from the pre-prepared Cellstar® 96-well plate. [38]

*Table 4. Composition of FURA buffer.*

| Material | Ingredients | Amount | Source |
|---|---|---|---|
| **10 X FURA buffer (pH = 7,2)** | NaCl | 40,3 g | Sigma- Aldrich (Vienna, Austria) |
| | KCl | 1,86 g | Sigma- Aldrich (Vienna, Austria) |
| | $MgCl_2$ anhydrous | 0,47 g | Sigma- Aldrich (Vienna, Austria) |
| | $CaCl_2 \times H_2O$ | 1,17 g | Sigma- Aldrich (Vienna, Austria) |
| | Glucose anhydrous | 5 g | Sigma- Aldrich (Vienna, Austria) |
| | HEPES (free acid) | 23,4 g | Sigma- Aldrich (Vienna, Austria) |
| | $ddH_2O$ | 500 ml | |
| **1 X FURA buffer** | 10 X FURA buffer | 50 ml | |
| | $ddH_2O$ | 450 ml | |

During the measurement the upper half of the plate was tested first and the lower half, still containing FURA buffer to prevent drying out of cells, later to avoid longer reaction time with the compounds. A fluorescence intensity scan was done with TECAN Spark® Microplate Reader. To measure emission of both fluorophores, CFP and Venus, a wavelength spectrum from 460 to 550 nm was chosen with a bandwidth of 20 nm.

### 4.1.1 Statistical Analysis

The results gathered by the TECAN Spark® Microplate Reader were then used to determine the mean values for the technical triplicates with Microsoft office excel. While the ratio between the fluorophores CFP/Venus was calculated, the values of the background from each compound were subtracted. This ensured that the recorded signals were solely from the cells. Next, the ratios were normalized to DMSO 0.1%, which was the baseline reference. Three independent biological experiments were conducted to assess the statistical significance of the results ($p$-value < 0.05). Statistical analyses were completed by a One-way-ANOVA test on the program GraphPad Prism 6.01. For substances that indicated potential antagonistic effects further testing was done in more concentrations to calculate the $IC_{50}$ value and create concentration-response curves by non-linear regression. [38]

## 5. Neutrophil Migration Assay

While *in vitro* experiments provided limited insight into therapeutic relevance, further functional testing was necessary to bridge the gap between controlled laboratory experiments and a more physiologically relevant response. With the findings from the EPAC assay, additional examinations were conducted to verify whether the potential antagonists showed similar effects on GPR84 expressed on neutrophils. Since the aim of this assay was to evaluate the ability of compounds to inhibit GPR84-dependent chemotaxis, fresh blood was required for the isolation of neutrophils. The Red Cross provided the necessary samples for the assay. Considering the rather short half-life (approximately a day) of neutrophils, the assay itself had to be completed in one day. [50]

The assay was divided into two main parts: seeding inserts and PMN (polymorphonuclear neutrophils) migration assay. To begin, Calu-3 cells were seeded onto ThinCert® Cell Culture inserts (Sarstedt, Germany) in 70 µl with a cell number of $0{,}2 \times 10^6$ cells per insert, the rest of the cell suspension was used to continue subculturing. Before pipetting that

volume onto each insert, they were laid upside down onto the bottom part of a 150 mm petri dish (Sarstedt, Germany) with a sterilized tweezer. After loading each ThinCert® Cell Culture insert with cells, the bottom part of another petri dish (Sarstedt, Germany) was used as a cover and put into the HERAcell® 150 incubator at 37 °C and 5% $CO_2$ overnight. On the next day, a Cellstar™ 24-well plate was prepared with 800 µl DMEM/F12 per well. Afterwards the overnight incubated ThinCert® Cell Culture inserts were taken out, inverted and transferred into the plate. Subsequently, 400 µl of DMEM/F12 was pipetted into the basolateral compartment of each ThinCert® Cell Culture insert and left in the HERAcell® 150 incubator at 37 °C and 5% $CO_2$ for 48 h. When the incubation period passed, another Cellstar™ 24-well plate was prepared with 800 µl DMEM/F12 per well to transfer the inserts from the old plate to the new one. By discarding the old media before the transfer, it could be replaced with new DMEM/F12. This ensured the steady growth of Calu-3 cells to eventually cover the surface of the membrane with a dense monolayer.

To monitor the formation of the barrier, the “Trans Epithelial Electrical Resistances” (TEER) values were measured every other day. By using an electrode, which was sterilized with ethanol before usage, one pole was dipped into the basolateral (insert) and the other into the apical (well) compartment. A low frequency current was applied to measure the resistance of the cell monolayer. If the barrier was dense, then the TEER values were higher, since Calu-3 cells disrupted the current flow. The primary focus was to achieve values >1000 Ω before further steps were initiated. [51,52] When the inserts reached those values, the next part of the migration assay could begin (**Figure 10**). All materials needed for the assay are listed in **Table 5**.

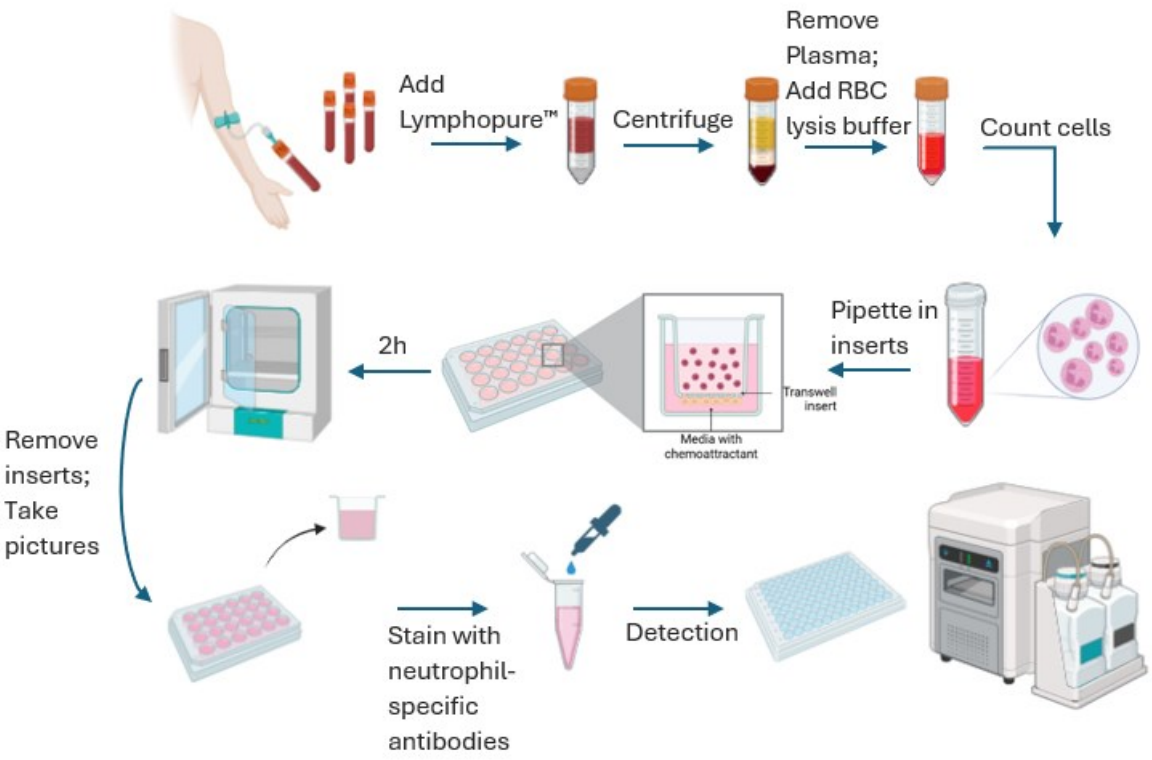


**Figure 10.** *Schematic overview of the neutrophil migration assay.*

When the ThinCert® Cell Culture inserts reach TEER values above 1000 Ω, neutrophils were isolated from fresh blood, which was provided by the Red Cross. After the treatment with Lymphopure™ and RBC lysis buffer a white pellet remained containing the PMN. The cell count was determined and subsequently resuspended in RPMI stripped + HEPES (pH = 7.2). Next, the cells were pipetted into the ThinCert® Cell Culture inserts and incubated for 2 hours. Once the incubation period passed, the ThinCert® Cell Culture inserts were removed, and images were taken of the wells to have a visual record of the migrated cells. To ensure that only neutrophils were counted during flow cytometry, the migrated cells were stained with neutrophil-specific antibodies prior to the measurement.

**RBC** = Red blood cells; Created with BioRender.com

*Table 5. Substances used for migration assay.*

| Material | Ingredients | Amount | Source |
|---|---|---|---|
| **DMEM/F12** | DMEM with phenol red 4,5 g/l glucose | 500 ml | Sigma-Aldrich (Vienna, Austria) |
| | Ham's F-12 Nutrient Mix | 500 ml | Sigma-Aldrich (Vienna, Austria) |
| | FBS | 2 x 50 ml | Gibco (Lofer, Austria) |
| | L-Glutamine (2 mM) | 2 x 5 ml | Lonza (Basel, Switzerland) |
| | Penicillin (100 U/ml) | 2 x 5 ml | Lonza (Basel, Switzerland) |
| | Streptomycin (100 µg/ml) | | |
| **10 X RBC lysis buffer (pH = 8)** | $NH_4Cl$ | 41,3 g | Sigma- Aldrich (Vienna, Austria) |
| | $NaHCO_3$ | 5 g | Sigma- Aldrich (Vienna, Austria) |
| | 0,5 M EDTA | 1 ml | Carl-Roth (Karlsruhe, Germany) |
| | $ddH_2O$ | 500 ml | |
| **1 X RBC lysis buffer** | 10 x RBC lysis buffer | 50 ml | |
| | $ddH_2O$ | 450 ml | |
| **RPMI stripped + HEPES (pH = 7.2)** | RPMI | 500 ml | Sigma- Aldrich (Vienna, Austria) |
| | Charcoal stripped FBS | 25 ml | Gibco (Lofer, Austria) |
| | HEPES (11 mM) | 1,4 g | Sigma- Aldrich (Vienna, Austria) |
| | L-Glutamine (2 mM) | 5 ml | Lonza (Basel, Switzerland) |
| | Penicillin (100 U/ml) | 5 ml | Lonza (Basel, Switzerland) |
| | Streptomycin(100 µg/ml) | | |
| **Staining solution** | CD45 (VioBlue) | 3 µl | Miltenyi Biotech (Gladbach, Germany) |
| | CD14 (APC) | 3 µl | Miltenyi Biotech (Gladbach, Germany) |
| | CD16 (PE Vio770) | 3 µl | Miltenyi Biotech (Gladbach, Germany) |
| | CD11b (APC Vio770) | 3 µl | Miltenyi Biotech (Gladbach, Germany) |
| | CD66b (FITC) | 3 µl | Miltenyi Biotech (Gladbach, Germany) |
| | PI (Propidium iodide) | 5 µl | Miltenyi Biotech (Gladbach, Germany) |
| | PFE buffer | 285 µl | |
| **PFE buffer** | PBS | 45 ml | |
| | FBS | 2,5 ml | Gibco (Lofer, Austria) |
| | 0,5 M EDTA | 200 µl | Carl-Roth (Karlsruhe, Germany) |

To begin, the neutrophils had to be isolated from the whole blood, so two 50 ml falcon tubes (Sarstedt, Germany) were filled equally with the obtained blood. PBS was used to dilute the blood in a 1:1 ratio to reduce viscosity. Another set of 50 ml falcon tubes (Sarstedt, Germany) was filled with 10 ml Lymphopure™. Subsequently, the diluted whole blood was layered carefully dropwise onto the Lymphopure™. After preparing everything, the tubes were centrifuged (Heraeus™ 1 S-R Multifuge, Germany) for 30 minutes at 500 g without any brakes as to not disturb the layers that were formed. Three layers were visible after the centrifugation was completed: yellow (top layer) → plasma, white → Lymphopure™ and red → red blood cells (RBC) and granulocytes. The yellow layer was gently removed via pipetting. Both falcon tubes (Sarstedt, Germany) were then filled up with RBC lysis buffer, which breaks down red blood cells while leaving granulocytes intact. They were again centrifuged (Heraeus™ 1 S-R Multifuge, Germany) for 5 minutes at 500 g. Afterwards, approximately 40 ml of the sample was transferred into another set of falcon tubes (Sarstedt, Germany) and all four tubes filled up again to 50 ml with RBC lysis buffer. They were then incubated for 5 minutes under the laminar airflow workbench HERAsafe®KS18, with constant inverting. Following this step, they were placed back into the centrifuge (Heraeus™ 1 S-R Multifuge, Germany) to spin with the same settings as before. The supernatant was discarded leaving solely 10 – 15 ml in the tubes, followed by filling them up to 50 ml with RBC lysis buffer and incubating them for 5 minutes and centrifugation. Next, the supernatant from all tubes was thrown away. The cell pellets were resuspended by using 5 ml RBC lysis buffer and combining them in one falcon tube (Sarstedt, Germany). One final cycle with the RBC lysis buffer incubation was performed. At this stage, a clear white pellet should be seen in the tube. After removing the supernatant, the cells were resuspended in PBS and counted via Vi-Cell™ XR cell viability Analyzer (Beckman Coulter, USA). The cells were again centrifuged so that PBS could be removed. The pellet was resuspended in RPMI stripped + HEPES (pH = 7.2) medium to achieve a density of $5 \times 10^6$ cells/ml. The next step was to prepare the compound dilutions at a 1:1000 ratio, using RPMI stripped + HEPES (pH = 7.2) medium. The first four wells served as controls: DMSO (0,2%), N-Formylmethionyl-leucyl-phenylalanine (fMLP) (10 nM), IL-8 (100 ng/ml) and Embelin (3 µM). The focus was to test for antagonistic effects during Embelin-induced, GPR84-dependent chemotaxis: therefore, a co-treatment with Embelin (3 µM) was performed. These compounds were pipetted into a Cellstar™ 24-well

plate. Then the ThinCert® Cell Culture inserts were transferred into the plate. The basolateral compartment was filled with 400 µl cell-suspension per insert. After finishing up the plate, it was put into the HERAcell® 150 incubator for 2 h at 37 °C and 5% $CO_2$ to allow cell migration. While the plate was being incubated, a staining solution was prepared using antibodies (CD45, CD14, CD16, CD11b and CD66b) at a 1:300 dilution in PFE buffer (PBS with FCS and EDTA) (**Table 6**). After the incubation period passed, the plate was taken out to remove the inserts. For visual recording the Cellstar™ 24-well plate was placed into the TECAN Spark® Microplate Reader. With the live camera function wells could be inspected, and images were taken. Next, the migrated PMNs were carefully resuspended and 500 µl aliquots were transferred into pre-labeled Eppendorf tubes. This was followed by a centrifuge cycle for 5 minutes at 5000 g. Subsequently, the resulting supernatant was carefully removed, and the cell pellet resuspended with 10 µl antibody staining solution. After a 30-minute incubation period, the Eppendorf tubes were filled to a total volume of 200 µl with PFE-buffer. The cell suspensions were then pipetted into a Cellstar® 96-well plate.

To determine the number of neutrophils having migrated through the barrier of Calu-3 cells, the cell numbers in the plate were measured via flow cytometry. Cells were gated based on forward and side scatter to exclude debris and doublets. Antibodies against CD45, CD14, CD16, CD11b, and CD66b were used to specifically identify viable granulocytes, with CD66b serving as a neutrophil-specific marker. This ensured that dead Calu-3 cells and other non-granulocytic remnants were excluded.

## 5.1 Statistical analysis

The results gathered from the measurement were processed in GraphPad Prism 6.01. Statistical comparison between groups was performed using One-way ANOVA. A *p*-value $< 0.05$ was considered statistically significant. For substances that indicated antagonistic effects further testing was done with different concentrations, to calculate the $IC_{50}$ values and create concentration-response curves by non-linear regression.

# D. Results

## 1. Results from CRE-Luciferase Assays

A target-based screening for TGR5 agonists was conducted with a range of substances from the DNTI project. To prove whether these compounds interact with TGR5, the intracellular cAMP levels were measured. Upon binding to this GPCR, the $G\alpha_s$ subunit activated adenylyl cyclase, leading to increased cAMP. This elevation results in a downstream anti-inflammatory reaction, or in this assay, to a CRE-dependent luciferase expression. [22]

### 1.1 Flavonoids

The first screening round identified three compounds as potential candidates for agonistic effects on TGR5. Further investigation identified these as flavonoids (**Figure 11**). Although their activity in TGR5 was higher compared to the other compounds, they were not specific for this receptor since the effect was also visible in the non-TGR5 expressing cell line EPAC HEK293 (**Figure 12**). The substances, DNTI 2796/2797/2798/2802 only differed by their substitution pattern and double bonds. Based on the assumption that this class of compounds may hold potential TGR5 agonists, the DNTI databank was combed through for more available flavonoids with similar structure and substitution patterns. A total number of 21 flavonoids were screened. Initially all compounds were assessed at 30 µM since higher concentrations were a risk for cytotoxicity. If potential agonists were found, further concentrations were evaluated to create a concentration-response curve.

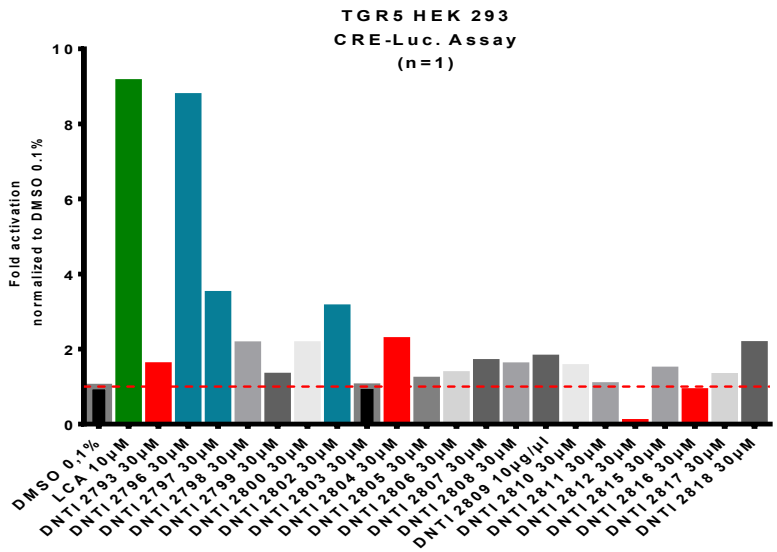


**Figure 11**. *Initial screening results of compounds from DNTI databank in TGR5 HEK 293 cells with the CRE-Luciferase assay.*

The graph shows the results from an initial screening of compounds from the DNTI project, tested at a concentration of 30 µM on TGR5 expressing HEK 293 cells. Three compounds (2796,2792,2802) showed potential agonistic behavior, indicated by prominent peaks. For the negative control, DMSO 0.1% was used, whereas lithocholic acid (LCA 10 µM) served as a positive control. Compounds with cytotoxic effects have been highlighted in red and potential hit compounds in blue. The data was analyzed with GraphPad Prism 6.01.
**DMSO** = Dimethyl sulfoxide; **LCA** = Lithocholic acid

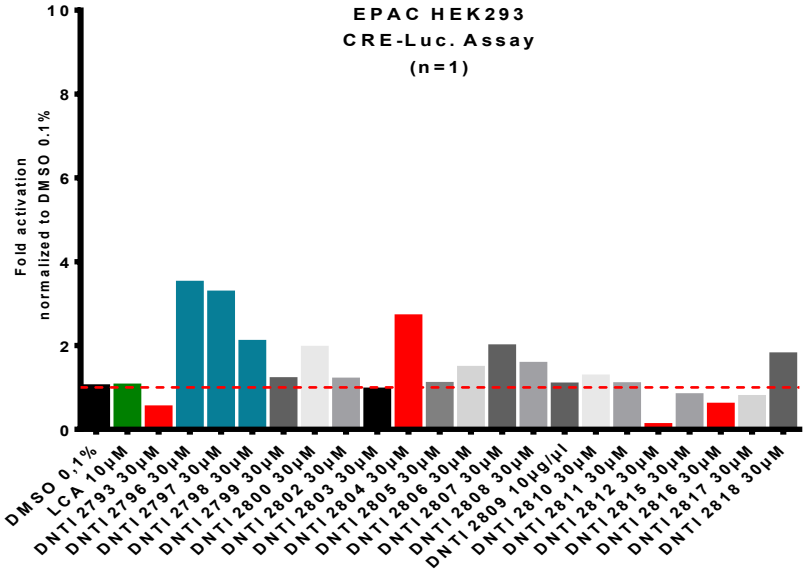


**Figure 12.** *Initial screening results of compounds from DNTI databank in non TGR5-expressing EPAC HEK 293 cells with the CRE-Luciferase assay.*

The graph shows the results from an initial screening of compounds from the DNTI project, tested at a concentration of 30 µM on non-TGR5 expressing EPAC HEK 293 cells. DMSO 0.1% was used as the negative control whereas LCA (10 µM) served as a positive control. Compounds with cytotoxic effects have been highlighted in red and potentially active compounds in blue. The data was analyzed with GraphPad Prism 6.01.
**DMSO** = Dimethyl sulfoxide; **LCA** = Lithocholic acid

During the testing process, a couple of flavonoids had to be excluded since the compounds ran out before repeated screenings were possible. Therefore only 15 substances remained, which could be tested in at least three biological replicates. Before analyzing the results, the compounds were divided into two groups depending on their core structure: one with double bond in Ring C (C2-C3) and ones without one (**Figure 13**).

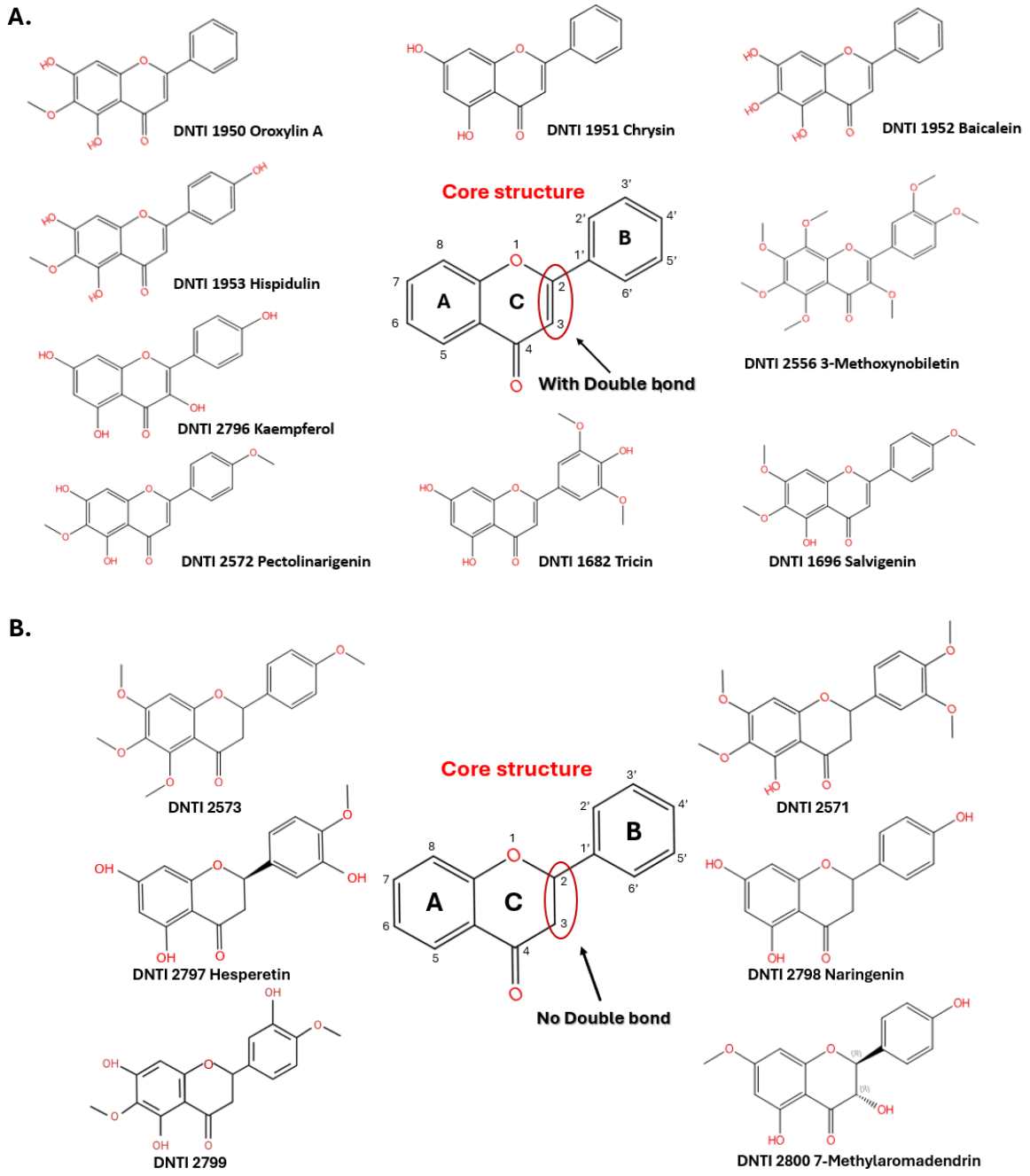


**Figure 13.** *Structures and names of flavonoids evaluated in CRE-Luciferase assay (Panels A-B). Structures retrieved and adapted from Scifinder (CAS) [73]*

This figure depicts the structures of the tested flavonoids in the CRE-Luciferase assay. Panel A shows all flavonoids with a double bond between C2 and C3 in ring C, whereas compounds from panel B lack this bond at the same position. CAS Registry Numbers for each flavonoid are provided in appendix (**Table 6**)

Even though an increase in intracellular cAMP levels was seen in nearly all the tested compounds, none of them showed specificity towards TGR5 when comparing the results with the ones obtained in non TGR5-expressing EPAC cells. To get more information on the degree of specificity, a selectivity-index was calculated. To obtain these values the following formular was used:

$$Selectivity\ Index = \frac{Mean\ fold\ activation\ in\ TGR5\ expressing\ cells}{Mean\ fold\ activation\ in\ non\ TGR5{-}expressing\ EPAC\ cells}.$$

The values indicated with what factor the compounds favor TGR5-mediated cAMP elevation over other potential signaling pathways also present in EPAC cells. Among the initial 15 flavonoids, two compounds, DNTI 2556 and 2571, demonstrated apparent functional selectivity towards TGR5 (**Figure 14**). However, their values were still less than half of that calculated for the positive control LCA (10 µM).

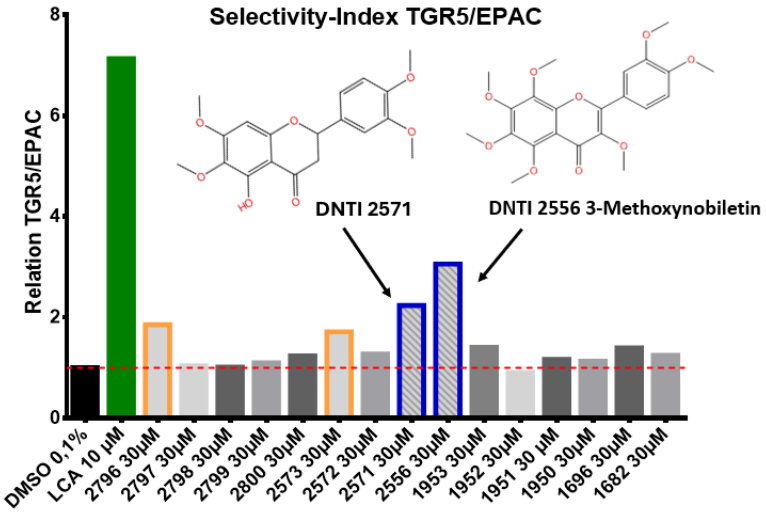


**Figure 14.** *Selectivity index (TGR5/EPAC) of tested flavonoids calculated from CRE-Luciferase assays.*

The index indicates the preference for each compound of activating TGR5 over the EPAC signaling pathway. Blue highlighted bars represent the flavonoids with a higher selectivity for TGR5. Two compounds (2571 and 2556) exhibited notable selectivity towards TGR5 but were still lower compared to the value of the positive control lithocholic acid (LCA 10 µM), which demonstrated the strongest preference. Additionally, two other flavonoids displayed a slight preference for TGR5, with selectivity indices around 2 (marked in orange).
**DMSO** = Dimethyl sulfoxide; **LCA** = Lithocholic acid

The results from the screening indicated that CRE-Luciferase activity was not only mediated by TGR5, since similar responses were identified in both TGR5 and non-TGR5 expressing cells. The substitution patterns on the core flavonoid structures, however, appeared to influence the effect on TGR5 and EPAC. The structure-dependent activities

were seen in both cell lines. For instance, modifying certain positions on ring A would either promote or diminish the effect of the compound, thus influencing the fold activation differently. This was seen with compounds 2797 and 2799, where substituting the hydrogen on position 6 of ring A with a methoxy group consequently led to reduced cAMP levels resulting in lower fold activation in both cell lines (**Figure 15**). A similar effect was observed for compounds 1951 and 1952, when the same position was replaced with a hydroxy group. Furthermore, replacing an existing methoxy group at position 7 on ring A with a hydroxy group, also decreased activity (**Figure 16**).

In contrast to substitutions on these suppressive positions on ring A, modifications on ring B, specifically on position 4', led to an increase of intracellular cAMP levels and intensified bioluminescence. By adding a hydroxy group at this position, more than doubled the signal, as demonstrated by compounds 1950 and 1953 (**Figure 17**).

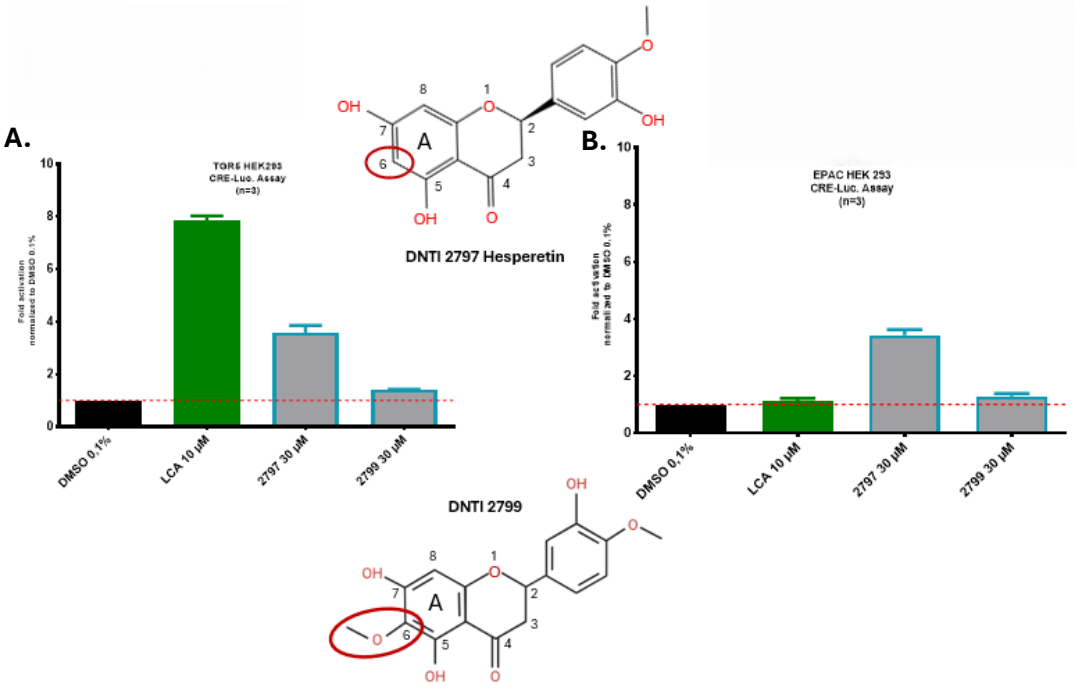


**Figure 15.** *Structure-dependent activity relationship of the flavonoids 2797 and 2799 in TGR5 (A) and EPAC (B) HEK cells using the CRE-Luciferase assay. Structure 2797 retrieved and adapted from Scifinder (CAS) [73]*

The structural difference between 2797 (Hesperetin, with hydrogen in position 6 on ring A) and 2799 (with a methoxy group in same position) are highlighted in red. The influence of this substitution was assessed using the CRE-Luciferase assay in TGR5 (A) and EPAC (B) HEK cells. The activities of the tested compounds are shown as mean values ± SD (standard deviation) of three biological replicates. The fold activation was normalized to negative control DMSO 0.1%. [38]

**DMSO** = Dimethyl sulfoxide; **LCA** = Lithocholic acid; Structure 2799 created with BioRender.com

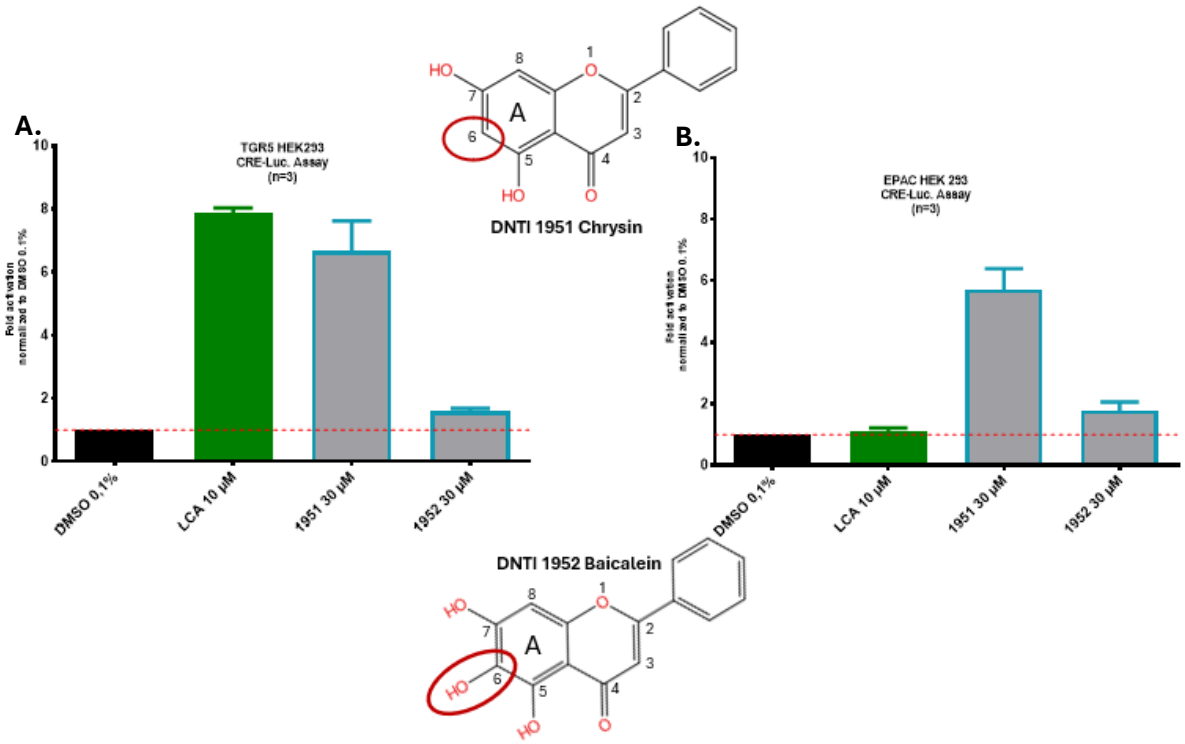


**Figure 16.** *Structure-specific activity relationship of compounds 1951 and 1952 in TGR5 (A) and EPAC (B) HEK cells using the CRE-Luciferase assay. Structures retrieved from Scifinder (CAS) [73]*

The structural difference between 1951 (Chrysin, with hydrogen at position 6 on ring A) and 1952 (Baicalein, with a hydroxy group in the same position) are highlighted in red. The influence of this substitution was assessed using CRE-Luciferase assay in TGR5 (A) and EPAC (B) HEK cells. The activities of the tested compounds are shown as mean values ± SD (standard deviation) of three biological replicates. The fold activation was normalized to negative control DMSO 0.1%. [38]
**DMSO** = Dimethyl sulfoxide; **LCA** = Lithocholic acid

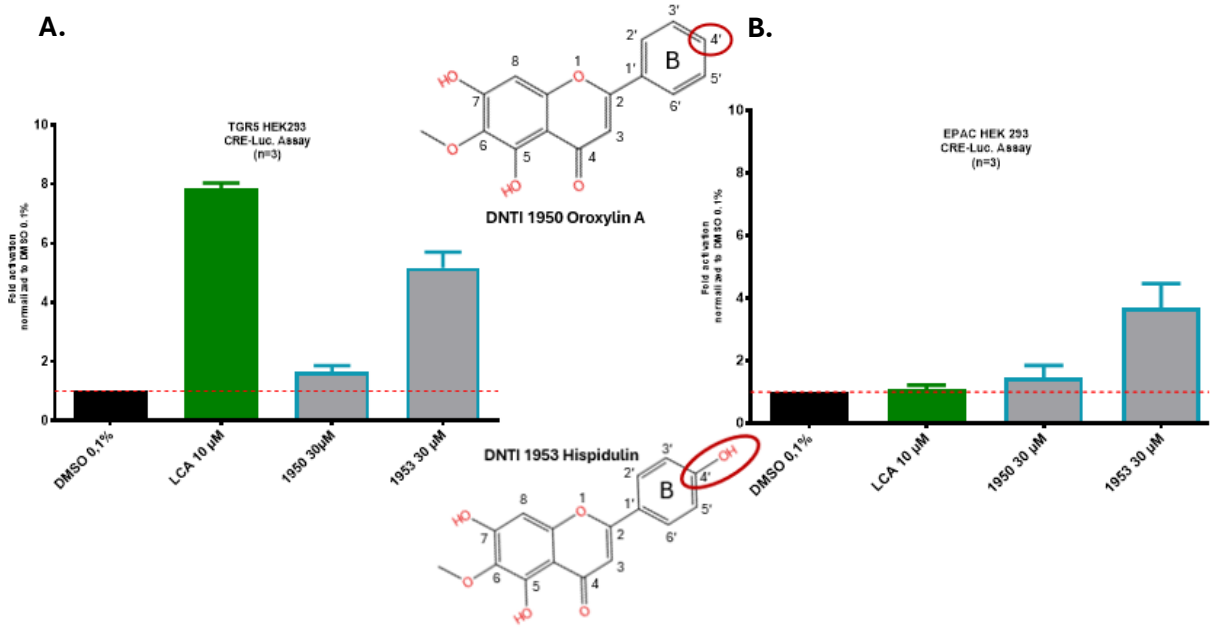


**Figure 17.** *Structure-specific activity relationship of compounds 1950 and 1953 in TGR5 (A) and EPAC (B) HEK cells using the CRE-Luciferase assay. Structures retrieved from Scifinder (CAS) [73]*

The structural difference between 1950 (Oroxylin A, with hydrogen in position 4' on ring B) and 1953 (Hispidulin, with a hydroxy group in same position) are highlighted in red. The influence from this substitution was assessed using CRE-Luciferase assay in TGR5 (A) and EPAC (B) HEK cells. The activities of the tested compounds are shown as mean values ± SD (standard deviation) of three biological replicates. The fold activation was normalized to negative control DMSO 0.1%. [38]
**DMSO** = Dimethyl sulfoxide; **LCA** = Lithocholic acid

## 1.2 Metabolites of flavonoids

While the batch of flavonoids showed no TGR5-specific activity during the screening, an alternative approach was explored. Flavonoids are metabolized by the gut microbiota most commonly into smaller phenolic acids like hydroxybenzoic, hydroxycinnamic and hydroxyphenylacetic acids. These microbial metabolites themselves exhibit effects such as promoting or inhibiting certain bacterial species therefore manipulating microbial diversity. [53–55]

Since TGR5 engages in regulating inflammation, it was hypothesized that microbial metabolites of flavonoids could show agonistic behavior toward this receptor, thereby modulating anti-inflammatory responses through downstream signaling.

The results detail whether the tested metabolites led to a TGR5-induced cAMP elevation and explore the specificity of these signals.

None of the screened substances exhibited cytotoxicity, so no influence on cell viability was detected under the testing conditions. The results from the fluorescence measurement for cell viability are included in the appendix. As indicated in **Figure 18**, none of the flavonoid metabolites led to a statistically significant elevation of intracellular cAMP levels. Their activity resembled that of the negative control, DMSO 0.1%. On the contrary, the screened flavonoids did demonstrate activation, however they were unspecific and not selective for the TGR5-mediated signaling pathway.

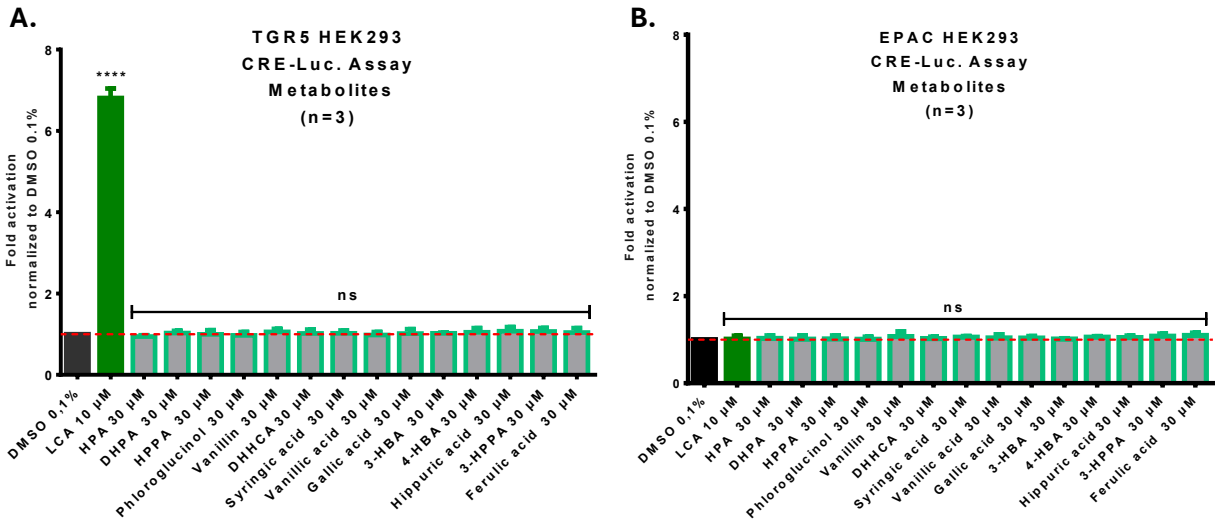


**Figure 18**. *Screening results of the flavonoid metabolites in TGR5 (A) and EPAC (B) HEK cells using the CRE-Luciferase assay.*

To determine the statistical significance, TGR5 and EPAC HEK cells were treated with the indicated compounds at a concentration of 30 µM. The results of the tested compound are shown as mean values ± SD of three biological replicates measured in technical quadruplicates. The statistical analysis was done by using a one-way-ANOVA analysis. The negative control was DMSO 0.1% and lithocholic acid (LCA 10 µM) was used as a positive control. [38]
Statistical significance evaluation: ****: $p \leq 0.0001$; ***: $p \leq 0.001$; **: $p \leq 0.01$; *: $p \leq 0.05$; ns: $p > 0.05$

**DMSO** = Dimethyl sulfoxide, **LCA** = Lithocholic acid, **HPA** = 3-Hydroxyphenylacetic acid, **DHPA** = 3,4-Dihydroxyphenylacetic acid, **HPPA** = 3-(4-Hydroxyphenyl)propionic acid, **DHHCA** = 3,4-Dihydroxyhydrocinnamic acid, **3-HBA** = 3-Hydroxybenzoic acid, **4-HBA** = 4-Hydroxybenzoic acid, **3-HPPA** = 3-(3-Hydroxyphenyl)propionic acid

## 1.3 Leoligin derivatives (DNTI compounds 2823/2826/2828)

The leoligin derivatives 2823, 2826 and 2828 were evaluated in the CRE-Luciferase assay for their potential TGR5-mediated cAMP elevation. An initial screening at a concentration of 30 µM with other substances (DNTI 2819-2832) showed higher fold activation values than the negative control (**Figure 19**). None of these substances exhibited pronounced cytotoxicity, as no influence on cell viability was detected under the testing conditions. The results from the fluorescence measurement as cell viability are included in the appendix. To determine a potential concentration-response relationship, further dilutions were tested.

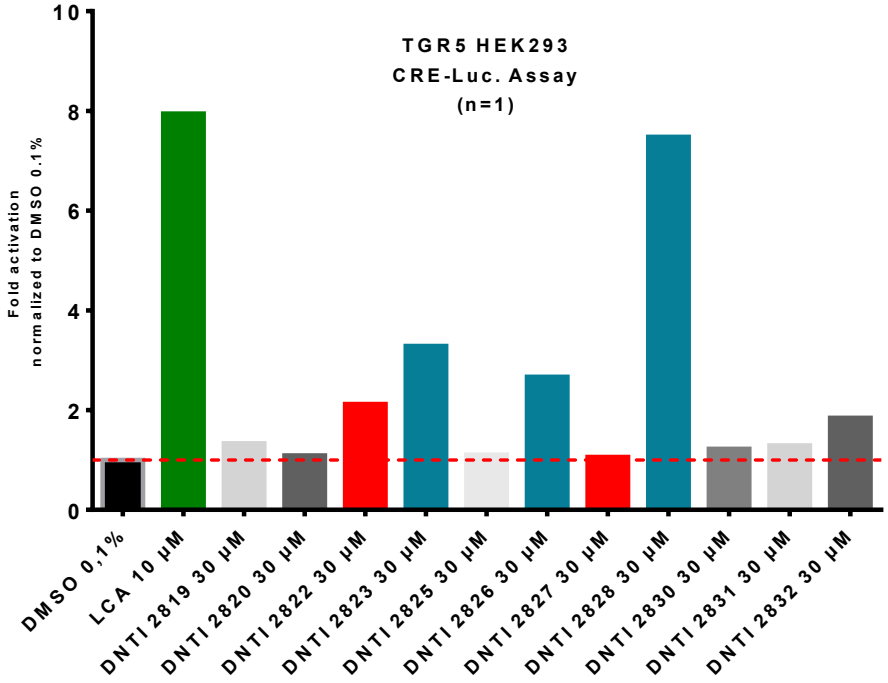


**Figure 19.** *Initial screening results of leoligin derivatives 2823/2826/2828 in TGR5 HEK293 cells in the CRE-Luciferase assay.*

The graph shows the results from an initial screening of compounds from the DNTI project, tested at a concentration of 30 µM on TGR5 expressing HEK 293 cells by CRE-Luciferase assay. Three compounds (2823, 2826, 2828) showed potential TGR5 agonistic behavior, indicated by their prominent peaks (blue). For the negative control DMSO 0.1% was used whereas LCA (10 µM) served as the positive control. Compounds with cytotoxic effects have been highlighted in red. The data was analyzed with GraphPad Prism 6.01.
**DMSO** = Dimethyl sulfoxide; **LCA** = Lithocholic acid

To begin with, compound 2823 was assessed in dilutions 30 - 1 µM, with DMSO as the solvent. The observed fold activations indicated a steady decline with decreasing concentrations and no more prominent activity at 1 µM. However, the activation through

this derivative was again not specific since an effect was also seen in the control EPAC HEK cell line (**Figure 20**).

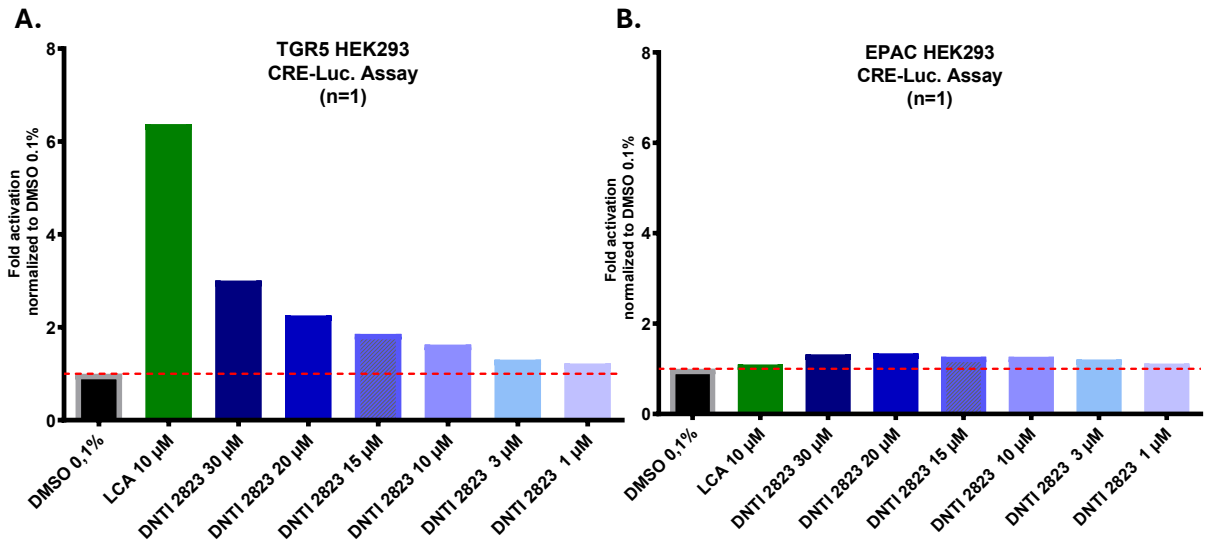


**Figure 20.** *Concentration-dependent activation of compound 2823 in TGR5 HEK (A) cells and EPAC HEK (B) cells using the CRE-Luciferase assay.*

The graph shows the fold activations of compound 2823 in different concentration ranging from 30 µM to 1 µM in TGR5 and EPAC HEK cells. The results were normalized to negative control DMSO 0.1%. Lithocholic acid (LCA 10 µM) served as a positive control. The data was analyzed with GraphPad Prism 6.01. This compound was tested in a single biological replicate (n=1) as a part of a preliminary sorting process. [38]
**DMSO** = Dimethyl sulfoxide; **LCA** = Lithocholic acid

For compounds 2826 and 2828 a different approach was explored. Firstly, three dilutions with a dilution factor of 1:3 were screened. With testing, it was determined whether any more dilutions were necessary to analyze the concentration-dependent response. As seen in **Figure 21A**, derivative 2826's activity was nearly gone by 3 µM so no further testing was done for this compound. With 2828 the decline of the signal was too abrupt from 30 µM to 10 µM, therefore more concentrations between these two concentrations were prepared to have a better understanding of the statistical significance in the fold activation and to create a potential concentration-response curve.

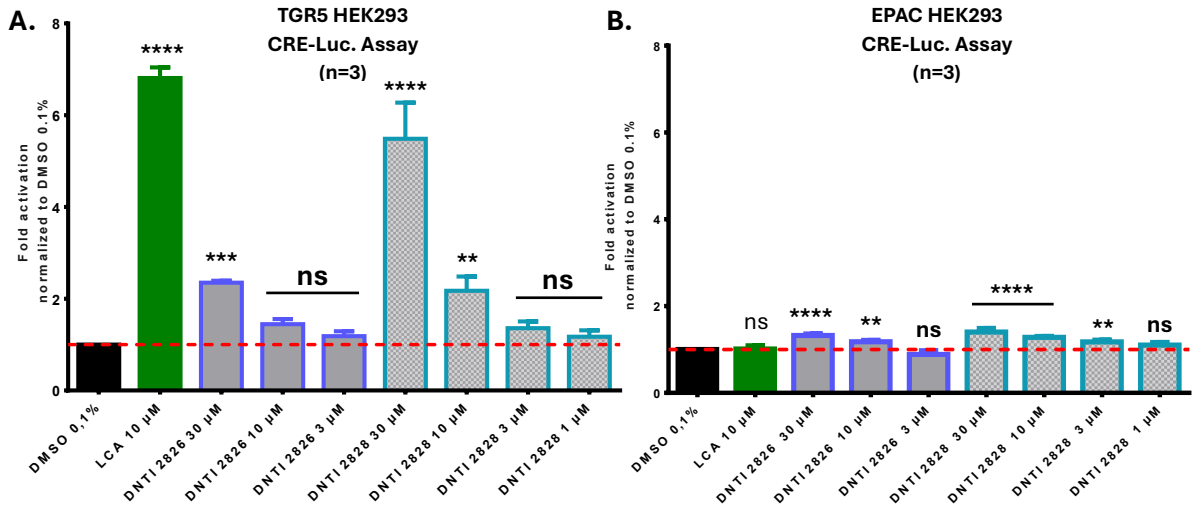


**Figure 21**. *Screening results of different concentrations of compounds 2826 and 2828 in TGR5 (A) and EPAC (B) cells using the CRE-Luciferase assay.*

To determine the statistical significance, TGR5 and EPAC HEK cells were treated with different concentrations (30/10/3/1 µM), respectively. The results of the tested compounds are shown as mean values ± SD of three biological replicates measured in technical quadruplicates. The statistical analysis was determined by using a one-way-ANOVA analysis. The negative control was DMSO 0.1% and LCA 10 µM was used as a positive control. [38]
Statistical significance evaluation: ****: $p \leq 0.0001$; ***: $p \leq 0.001$; **: $p \leq 0.01$; *: $p \leq 0.05$; ns: $p > 0.05$
**DMSO** = Dimethyl sulfoxide; **LCA** = Lithocholic acid

To evaluate the biological activity of the leoligin derivative 2828, three biological replicates were conducted after preparing the dilutions. Fold activations were normalized to the negative control (DMSO 0.1%) and the results were analyzed with a one-way ANOVA to determine statistical significance. As seen in **Figure 22A**, a concentration-dependent decline in activation was observed.

With the gathered results, a concentration-response curve was generated. While evaluating the data, it was observed that the values did not align well with a standard sigmoidal curve, thus, only an apparent $EC_{50}$ value of 17.3 µM could be determined (**Figure 22B**).

A.

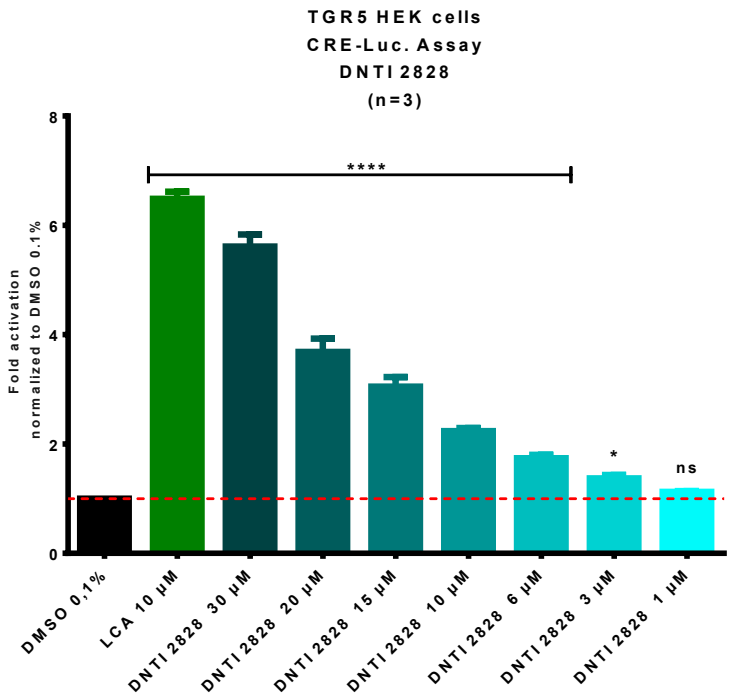


B.

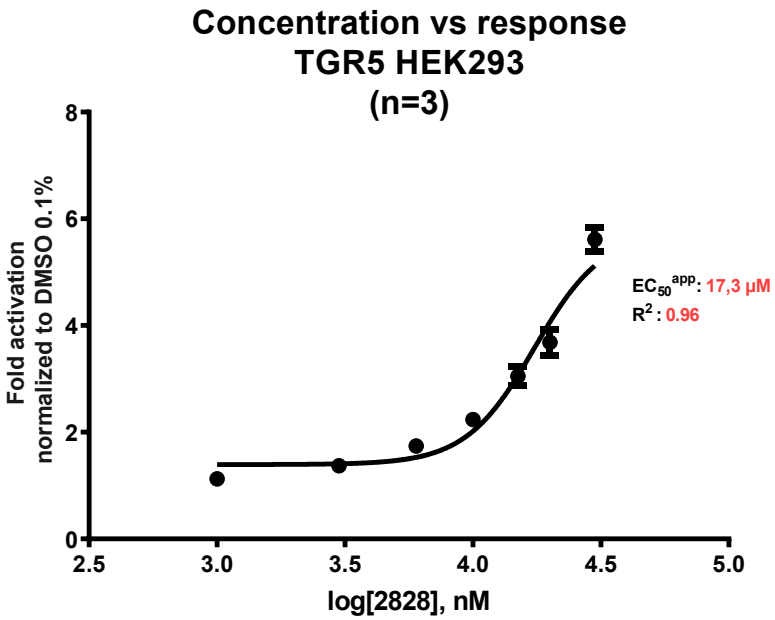


**Figure 22.** *Testing of different concentrations of compound 2828 in TGR5 HEK cells (A) and concentration-response curve (B) for 2828 using the CRE-Luciferase assay.*

(A) To determine the statistical significance of the effects of compound 2828 in CRE-Luciferase assays, TGR5 HEK cells were treated with different concentrations ranging from 30 µM to 1 µM. The results of the tested compound are shown as mean values ± SD (standard deviation) of three biological replicates measured in technical quadruplicates. The statistical analysis was performed by one-way-ANOVA analysis. The negative control was DMSO 0.1% while lithocholic acid (LCA 10 µM) was used as the positive control. Statistical significance evaluation: ****: $p \leq 0.0001$; ***: $p \leq 0.001$; **: $p \leq 0.01$; *: $p \leq 0.05$; ns: $p > 0.05$ [38]

(B) A concentration-dependent increase of intracellular cAMP levels by leoligin derivative 2828 was observed in three independent experiments by CRE-Luciferase assays. The results are shown as the fold activation normalized to the negative control DMSO 0.1%. The software GraphPad Prism 6.01 was used for the nonlinear regression analysis to calculate apparent $EC_{50}$ value of 17.3 µM with a $R^2$ value of 0.96. [38]

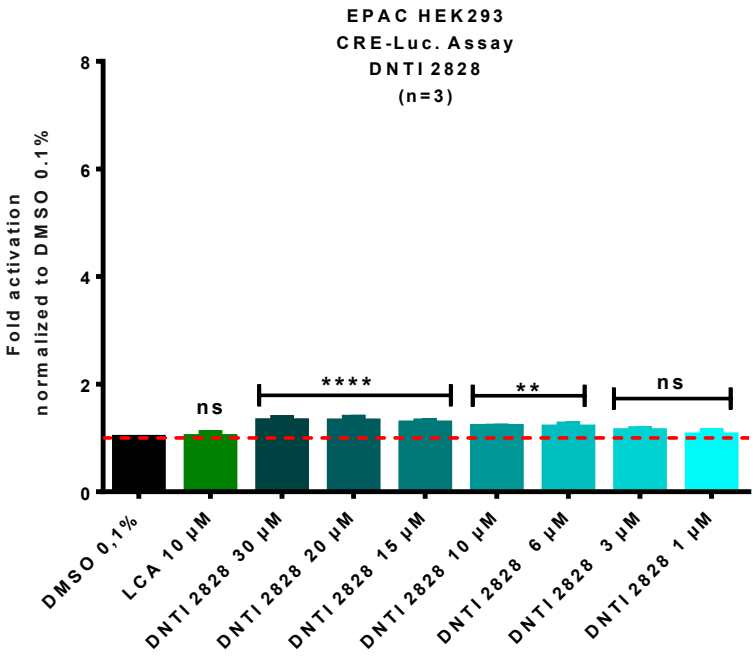


**Figure 23.** *Testing of different concentrations of compound 2828 in non-TGR5 expressing EPAC HEK cell line using the CRE-Luciferase assay.*

To determine the specificity of the activities of compound 2828, non-TGR5 expressing EPAC HEK cells were treated with different concentrations ranging from 30 µM to 1 µM. The results of the tested compound are shown as mean values ± SD of three biological replicates measured in technical quadruplicates. The statistical analysis was done by using a one-way-ANOVA analysis. The negative control was DMSO 0.1% and LCA 10 µM was used as a positive control. [38]
Statistical significance evaluation: ****: $p \leq 0.0001$; ***: $p \leq 0.001$; **: $p \leq 0.01$; *: $p \leq 0.05$; ns: $p > 0.05$
**DMSO** = Dimethyl sulfoxide; **LCA** = Lithocholic acid

Even though the TGR5-mediated cAMP elevation remained statistically significant up to a concentration of 1 µM, a significant increase (p-value < 0.05) of intracellular cAMP was also observed in non-TGR5 expressing cells up to a concentration of 6 µM (**Figure 22,23**). These overlapping effects are grounds for questioning the TGR5 specificity of compound 2828. However, a cAMP accumulating effect in cells remains evident, as demonstrated by the measurements.

## 2. Results from EPAC Assay

A target-based screening for GPR84 antagonists was performed with a range of substances from the DNTI project. To investigate whether these compounds interact with the GPR84 receptor, the intracellular cAMP levels were measured with an EPAC FRET biosensor. Upon ligand binding, the dissociation of the $G\alpha_i$ subunit leads to the inhibition of adenylyl cyclase and a decrease in cAMP levels. However, the presence of an GPR84 antagonist disrupts this process by blocking the inhibitory signal and instead leads to increased cAMP levels. This elevation results in a disrupted downstream pro-inflammatory signaling, or in this assay, to the absence of FRET between the fluorophore donor CFP and the acceptor fluorophore Venus. [34]

Three independent biological experiments were conducted to assess the statistical significance of the compounds with potential antagonistic effects ($p$-value $< 0.05$) .

### 2.1 Initial screening results

The first screening revealed five compounds as potential candidates for antagonistic effects on GPR84. Further investigation showed that these compounds comprise Leoligin (2819/2820/2823) and neolignane derivatives (2815/2817). Substance 2811 was not further tested since the increase of cAMP concentration was more intense in non-GPR84 expressing cells and therefore non-specific (**Figure 24**).

#### 2.1.1 Leoligin Derivatives

For the compounds 2819/2820/2823, it was observed that the intensity of the fluorescence-emission ratio lay either in or above the Forskolin-Embelin co-treatment range (**Figure 24, 25A**). Therefore, more dilutions were prepared to assess a potential concentration-dependent response.

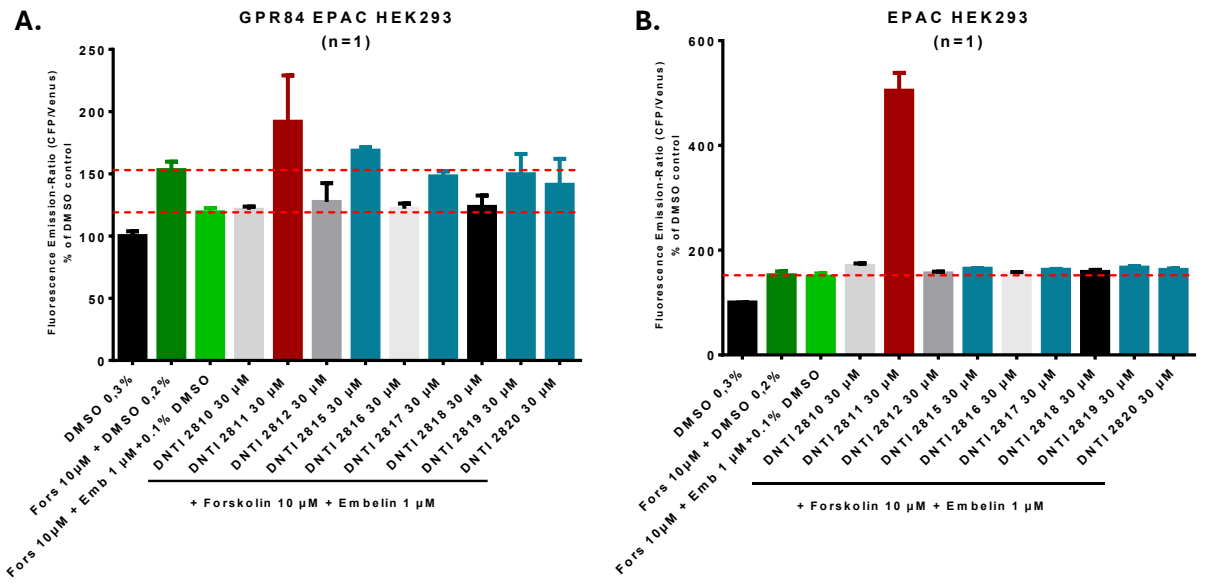


**Figure 24.** *Initial screening results of compounds from the DNTI project in GPR84 (A) and EPAC (B) HEK cells using the EPAC assay.*

The figure shows the measurement of intracellular cAMP levels, represented by the fluorescence emission ratio, in GPR84 and EPAC HEK cells after compound treatment. The graphs represent the means ± SD from technical triplicates. They were normalized to the negative control DMSO 0.3%. Compounds were used in co-treatment with Forskolin (10 µM) and Embelin (1 µM) to identify potential antagonists. Forskolin (10 µM) + DMSO 0.2% served as the upper reference for cAMP concentrations while Forskolin (10 µM) + Embelin (1 µM) + DMSO 0.1% represented the lower limit. The blue highlighted bars indicate compounds chosen for further testing. Substances that showed a high fluorescence emission ratio in both cell lines (marked in red) were excluded from further screening.
**DMSO** = Dimethyl sulfoxide; **Emb** = Embelin; **Fors** = Forskolin

To begin with, all potential hit compounds were assessed at a concentration of 30 µM and 10 µM. First, 2820 was eliminated from further experiments, since the effect was too weak at 10 µM (**Figure 25A**). Next, substance 2823, as seen in **Figure 25B**, was also observed as a potential antagonist but when tested at 10 µM, it lost its intensity and was therefore also excluded. Lastly, derivative 2819 (**Figure 25B**) and 2817 were excluded from future testing process as its signal was on the lower end of the Forskolin-Embelin range.

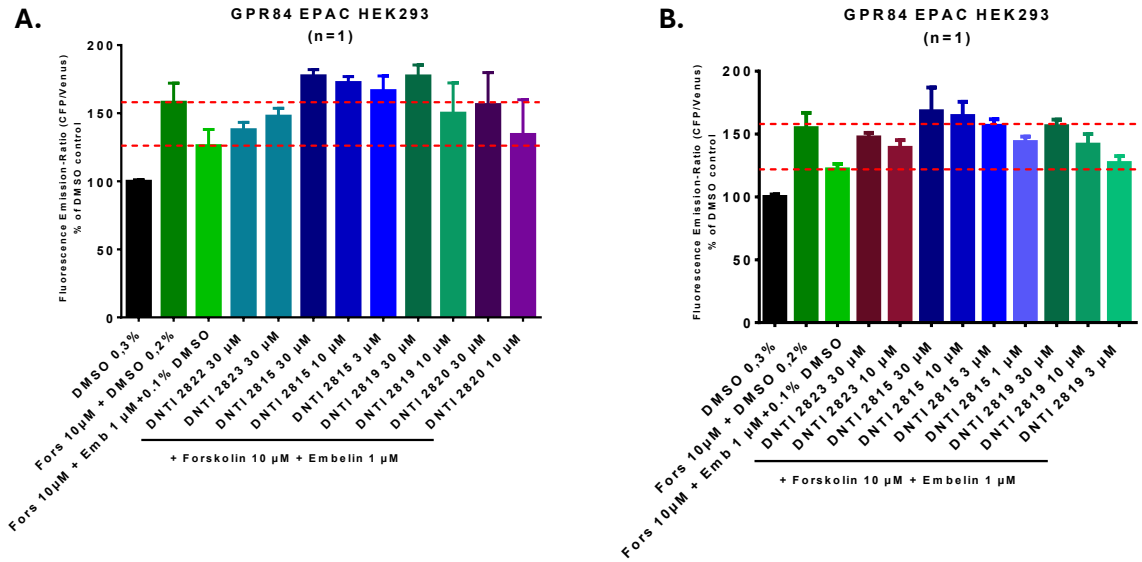


**Figure 25A and B.** *Results showing potential concentration-dependent effects of putative GPR84 antagonists in GPR84 HEK cells.*

The figure shows the concentration-dependent fluorescence emission ratios of the compounds from the initial screening (see **Figure 14**). The compounds were first tested at 30 µM and 10 µM (A). If the emission signal was still visible within the defined range (red dotted lines), it was further tested at 3 µM (B). The results of the tested compounds are shown as mean values ± SD of technical quadruplicates. Fluorescence emission ratios were normalized to the vehicle control DMSO. The dark green highlighted bar represents the control Forskolin (10 µM) + DMSO while the light green bar indicates Forskolin (10 µM) + Embelin (1 µM) + DMSO (0.1%).
**DMSO** = Dimethyl sulfoxide; **Emb** = Embelin; **Fors** = Forskolin

### 2.1.2 Neolignane derivatives

In the EPAC assay both derivatives, 2815 and 2817, increased intracellular cAMP levels suggesting a potential as GPR84 antagonists. Upon further testing it was observed that the fluorescence emission ratio was at its lowest for 2817 by 3 µM. However derivative 2815 showed a signal higher than the embelin 1 µM control (**Figure 25B**). Therefore, more tests were conducted with compound 2815.

#### 2.1.2.1 Determination of the antagonistic activity of derivative 2815

After the screening for potential GPR84 antagonists, neolignane derivate 2815 remained the sole candidate with elevated cAMP levels down to a concentration of 1 µM. Subsequently, a dilutions series ranging from 30 µM down to 3 nM was prepared. Each concentration was tested in three biological replicates to determine the statistical significance and the $IC_{50}$ value, which was found to be 565.8 nM ($R^2$ = 0.69). As shown in **Figure 26A,** the significance was evaluated by a one-way ANOVA with Dunnett's post hoc test against the control "Forskolin (10 µM) + Embelin (1 µM) + DMSO 0.1%", which showed the lowest cAMP levels due to GPR84 antagonism of Embelin. The vehicle control DMSO

0.1% was not used for comparison since it was confirmed previously that the solvent itself did not affect the assay.

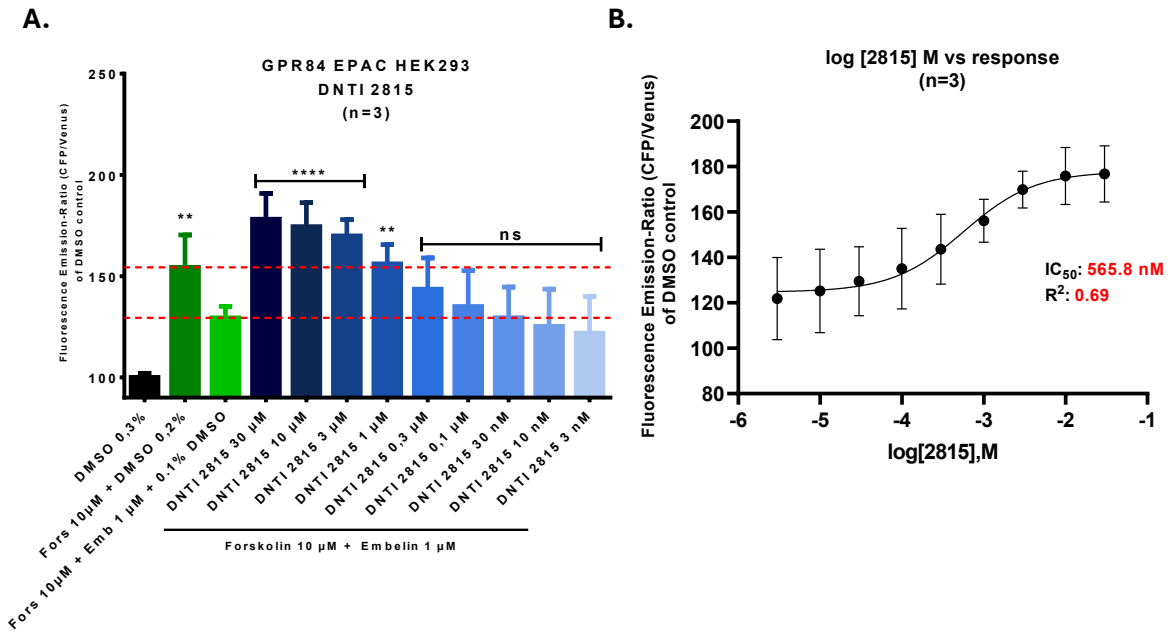


**Figure 26.** *Concentration-dependent GPR84 antagonistic activity of compound 2815 (A) and concentration-response curve (B).*

(A) To determine the statistical significance of the effects of 2815, GPR84 HEK cells were treated with different concentrations of 2815 ranging from 30 µM to 3 nM. The results of the tested compound are shown as mean values ± SD (standard deviation) of three biological replicates, each measured in technical triplicates in the EPAC assay. The statistical analysis was performed by one-way-ANOVA analysis. The negative control was DMSO 0.1% while Forskolin (10 µM) and Forskolin (10 µM) + Embelin (1 µM) were used as a reference for the range of target cAMP levels (indicated by red dotted lines). [38]
Statistical significance evaluation: ****: $p \leq 0.0001$; ***: $p \leq 0.001$; **: $p \leq 0.01$; *: $p \leq 0.05$; ns: $p > 0.05$ [38]

(B) A concentration-dependent increase of intracellular cAMP levels by the derivative 2815 was observed in three independent measurements. The data is shown as the fluorescence emission ratio (CFP/Venus) normalized to the negative control DMSO 0.1%. The software GraphPad Prism 6.01 was used for the nonlinear regression analysis to calculate an apparent $IC_{50}$ value of 565.8 nM (0.566 µM) with a $R^2$ value of 0.69. [38]
**DMSO** = Dimethyl sulfoxide; **Emb** = Embelin; **Fors** = Forskolin

To investigate whether the antagonistic behavior was specific for GPR84, a dilution series was tested in the assay under various conditions. First, the compound was screened without Forskolin/Embelin co-treatment. Under these conditions, no cAMP elevation was detected including the non-GPR84 expressing EPAC cell line, suggesting a specificity for GPR84 (**Figure 27A** and **B**). All concentrations showed similar activity to the negative control DMSO 0.1%, leading to the hypothesis that Forskolin, Embelin and GPR84 were necessary for compound 2815 to elevate the intracellular cAMP levels. Next, the dilution series was evaluated with Forskolin (10 µM) co-treatment. Here, an increase of cAMP levels across all concentrations was observed in both GPR84 and in non-GPR84

expressing cells (**Figure 27C** and **D**). This finding refuted the earlier hypothesis of needing GPR84 receptor expression, Forskolin and Embelin for a cAMP-elevating effect by compound 2815 and that it may be due to some off-targets or GPR84-independent mechanisms.

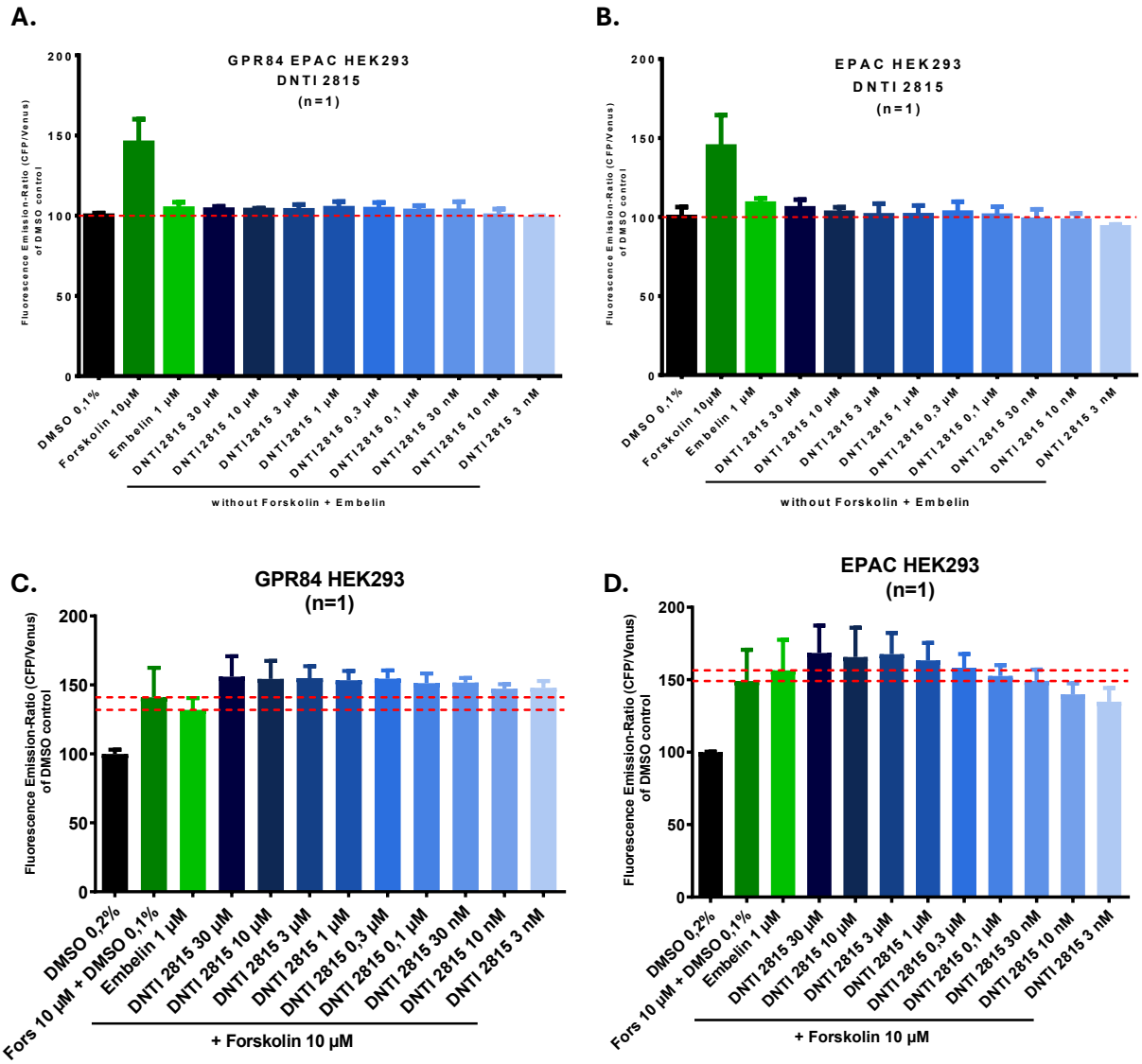


**Figure 27.** *Results of a compound 2815 dilution-series of in the EPAC assay under different assay conditions (Panels A-D).*

The figure shows the fluorescence emission ratios after compound 2815 treatment in GPR84-expressing and non-expressing cells under varying assay conditions. The results of the tested compound are shown as mean values ± SD of technical quadruplicates. Fluorescence emission ratios were normalized to the vehicle control DMSO.

A,B: Results of the dilution series without the Forskolin (10 µM) + Embelin (1 µM) co-treatment. The dark green highlighted bar represents the control Forskolin (10 µM), while the light green bar indicates Embelin (1 µM).

C,D: Results of compound dilutions with Forskolin (10 µM) co-treatment. The dark green highlighted bar represents the control Forskolin (10 µM) + DMSO while the light green bar indicates Forskolin (10 µM) + Embelin (1 µM).

## 3. Neutrophil-Migration Assay

To continue exploring the therapeutic potential of identified GPR84 antagonists, experiments were conducted under conditions more closely resembling pathological and physiological responses.

GPR84 is commonly expressed on neutrophils, immune cells involved in initiating the innate immune reactions. Through the activation of GPR84 with agonists such as medium-chain fatty acids and Embelin, a GPR84-dependent chemotaxis is triggered, resulting in the migration of neutrophils towards sites of infection. [20,32,33,48] To experimentally simulate this mechanism, Calu-3 cells were cultured on ThinCert® Cell Culture inserts to form a monolayer and placed onto a CellStar™ 24-well plate filled with chemotactic compounds. Into the basolateral compartment, the freshly isolated neutrophils were pipetted and incubated to achieve a GPR84-mediated migration. The primary aim was to evaluate an antagonistic behavior during Embelin-induced, GPR84-dependent chemotaxis. Thus, a co-treatment of potential antagonists with Embelin (3 µM) in the apical compartment was conducted to assess their impact on PMN migration. The migrated cells were visualized through images taken with the TECAN Spark® Microplate Reader to monitor the cells.

Three independent biological experiments were conducted to assess the statistical significance of the results (p-value < 0.05). Quantification was performed by flow cytometry. For each compound, the mean PMN count, and standard deviation (SD) were calculated. If potential antagonistic behavior was observed during testing, a dilution series was prepared to determine a potential concentration-response curve by non-linear regression and $IC_{50}$ values were calculated.

### 3.1 Initial results

First, all potential antagonists identified in the EPAC assay were tested on freshly isolated neutrophils to determine if the effects could also be seen in the migration assay. After eliminating inactive compounds based on the extent of migrated neutrophils (data not shown), four compounds (1721, 2412, 2815, 2819) remained for further evaluation (**Figure 28**).

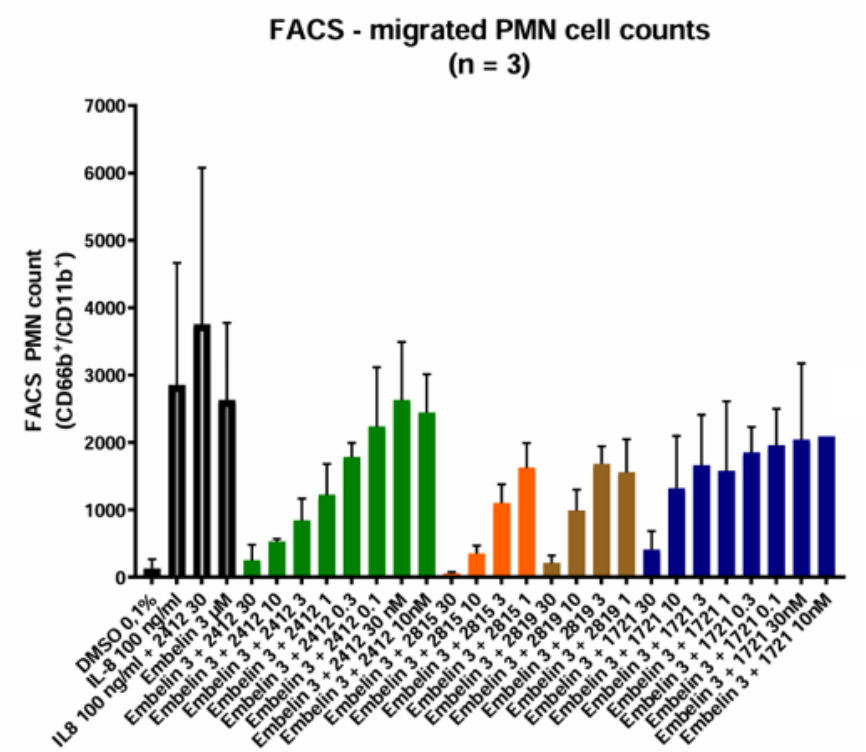


**Figure 28.** *Overview of the results obtained in the PMN migration assay in response to compound treatment.*

The figure depicts all tested compounds in the migration assay. All compounds were co-treated with Embelin (3 µM), a known GPR84 agonist and the data represent the mean ± SD (standard deviation) of PMN counts determined by FACS analysis from three independent biological replicates. A concentration-dependent effect can be seen in all tested compounds. Black highlighted bars represent the negative control DMSO 0.1%, IL-8 (100 ng/ml), IL-8 (100 ng/ml) + 2412 (30 µM) and positive control Embelin (3 µM). **DMSO** = Dimethyl sulfoxide

### 3.1.1 Compounds 2815 & 2819

Compounds 2815 and 2819 were assessed in up to three biological replicates at concentrations ranging from 30 µM to 1 µM. While both displayed promising activity in the EPAC assay, the same was not observed in the PMN migration assay. The inhibitory effect declined rapidly with decreasing concentrations and even though the concentration-response curves could be fitted, neither compound demonstrated a defined lower or upper plateau.

Neolignane derivative 2815 had an estimated $IC_{50}$ value of 2.6 µM with an $R^2$ value of 0.93, while the leoligin derivative 2819 showed an $IC_{50}$ value of 24 µM and an $R^2$ of 0.84. Due to their limited inhibitory effects further testing was discontinued (**Figure 29,30**). Therefore, further screenings focused on synthetic compound 1721 and Imbricaric acid (compound 2412), which underwent comprehensive concentration-response analysis.

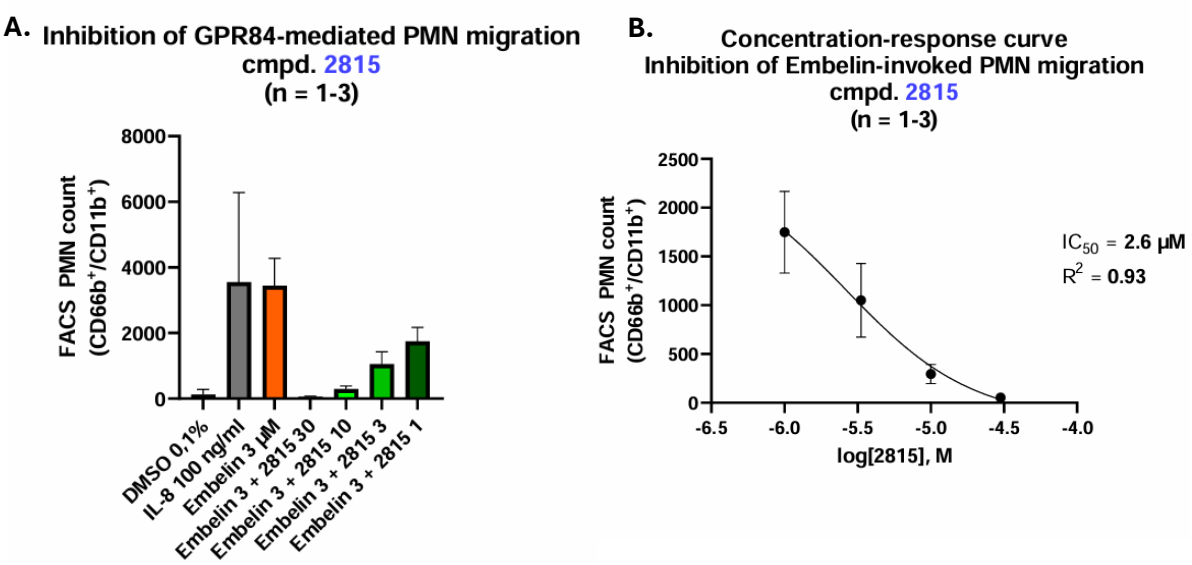


**Figure 29.** *Results of compound 2815 in the PMN migration assay (A) and concentration-response curve (B).*

**(A)**: To determine the effects of 2815 in the PMN migration assay, the freshly isolated neutrophils were co-treated with different concentrations of 2815 ranging from 30 µM to 1 µM with Embelin (3 µM). The results of the tested compound are shown as mean values ± SD (standard deviation) of three biological replicates. The negative control was DMSO 0.1% while IL-8 (100 ng/ml) and Embelin (3 µM) were used as a reference
**(B)**: A concentration-dependent reduction of the migrated neutrophils by derivative 2815 was determined in three independent measurements. The data is shown as the PMN count determined with neutrophil specific antibodies CD66b/CD11b in FACS analysis. The software GraphPad Prism 6.01 was used for the nonlinear regression analysis to calculate an apparent $IC_{50}$ value of 2.6 µM with a $R^2$ value of 0.93. [38]

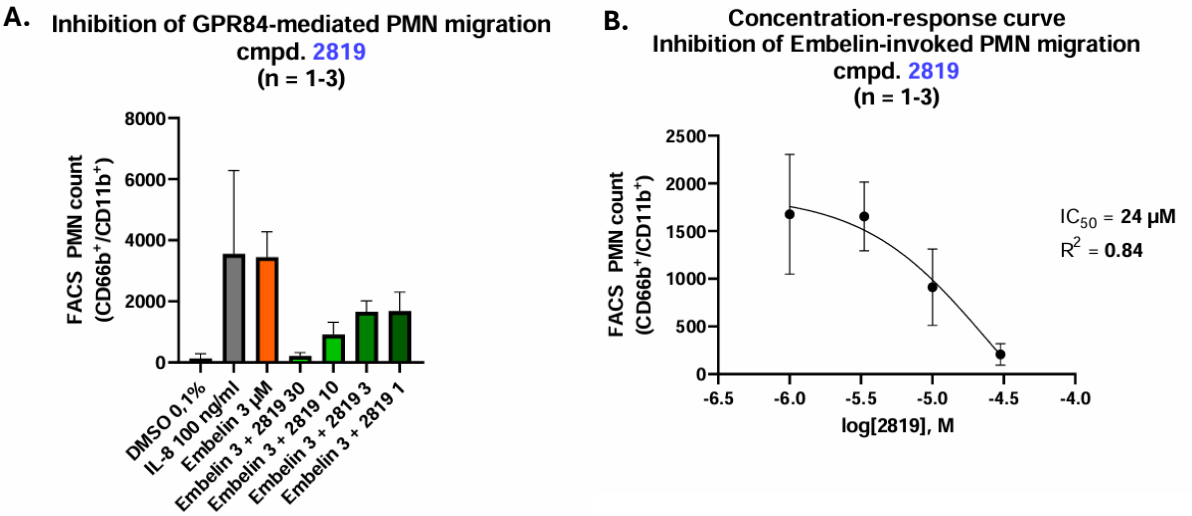


**Figure 30.** *Results of compound 2819 in the PMN migration assay (A) and concentration-response curve (B).*

**(A)** To determine the effects of 2819 in the PMN migration assay, the freshly isolated neutrophils were co-treated with different concentrations of 2819 ranging from 30 µM to 1 µM with Embelin (3 µM). The results of the tested compound are shown as mean values ± SD (standard deviation) of three biological replicates. The negative control was DMSO 0.1% while IL-8 (100 ng/ml) and Embelin (3 µM) were used as a reference.
**(B)**: A concentration-dependent reduction of the migrated neutrophils by compound 2819 was determined in three independent measurements. The data is shown as the PMN count determined with neutrophil specific antibodies CD66b/CD11b in FACS analysis. The software GraphPad Prism 6.01 was used for the nonlinear regression analysis to calculate an apparent $IC_{50}$ value of 24 µM with a $R^2$ value of 0.84. [38]

### 3.1.2 Compound 1721

The synthetic compound 1721 is a commercially available substance and was initially screened by a previous student in the EPAC assay. Although showing promising effects in the in- vitro experiments the same was not observed in the neutrophil migration assay. To evaluate the biological activity of 1721, three independent experiments were conducted in concentrations ranging from 30 µM to 0.1 µM. The results were analyzed with a one-way ANOVA to determine statistical significance. Aside from 30 µM, no other concentration indicated statistical significance, when compared to control Embelin (3 µM) alone (**Figure 31A**). After completing the third replication, no clear activity was seen in the results lowering the interest in this compound.

With the gathered results, a concentration-response curve was generated. While evaluating the data, it was observed that the values did not align well with a standard sigmoidal curve, thus, only an apparent $IC_{50}$ value of 63 µM with only an R value of 0.48 was determined, indicating the concentration at which half of the maximal activation was exhibited (**Figure 31B**).

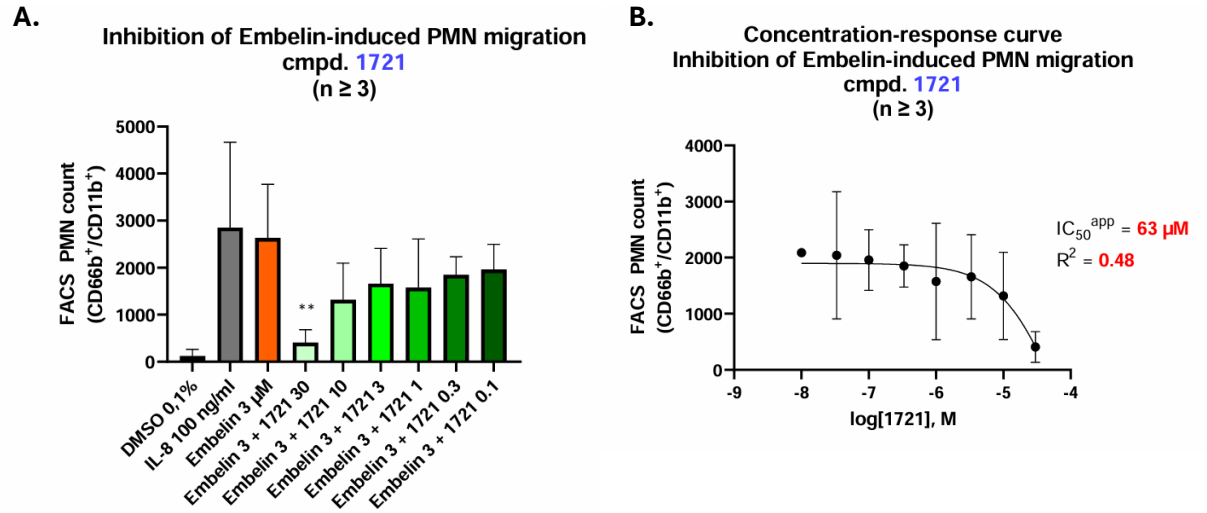


**Figure 31.** *Results of compound 1721 in the PMN migration assay (A) and concentration-response curve (B).*

**(A)** To determine the statistical significance of the effects of 1721 in the PMN migration assay, the freshly isolated neutrophils were co-treated with different concentrations of 1721 ranging from 30 µM to 0.1 µM with Embelin (3 µM). The results of the tested compound are shown as mean values ± SD (standard deviation) of three biological replicates. The statistical analysis was performed by one-way-ANOVA analysis. The negative control was DMSO 0.1% while IL-8 (100 ng/ml) and Embelin (3 µM) were used as a reference. [38]
Statistical significance evaluation: ****: $p \leq 0.0001$; ***: $p \leq 0.001$; **: $p \leq 0.01$; *: $p \leq 0.05$; ns: $p > 0.05$
**(B):** A concentration-dependent reduction of the migrated neutrophils by compound 1721 was determined in three independent measurements. The data is shown as the PMN count determined with neutrophil specific antibodies $CD66b^+/CD11b^+$ in FACS analysis. The software GraphPad Prism 6.01 was used for the nonlinear regression analysis to calculate an apparent $IC_{50}$ value of 63 µM with a $R^2$ value of 0.48. [38]

### 3.1.3 Imbricaric acid (2412)

Out of all the tested compounds from the DNTI project, Imbricaric acid (2412) showed the most promising antagonistic properties towards GPR84 and its role in inhibiting neutrophil (PMN) migration. Previously assessed using the EPAC assay by a former master student, this study continued the investigation to deepen the understanding of compound 2412's effect on GPR84-mediated PMN migration.

A concentration-response experiment was performed using dilutions ranging from 30 µM to 10 nM. Following three biological replicates (n ≥ 3), the results indicated a statistically significant ($p < 0.05$) reduction in neutrophil migration at concentrations as low as 1 µM. The generated concentration-response curve represented a typical sigmoidal shape with an $IC_{50}$ value of 698 nM ($R^2 = 0.75$), indicating potent inhibitory activity (**Figure 32**).

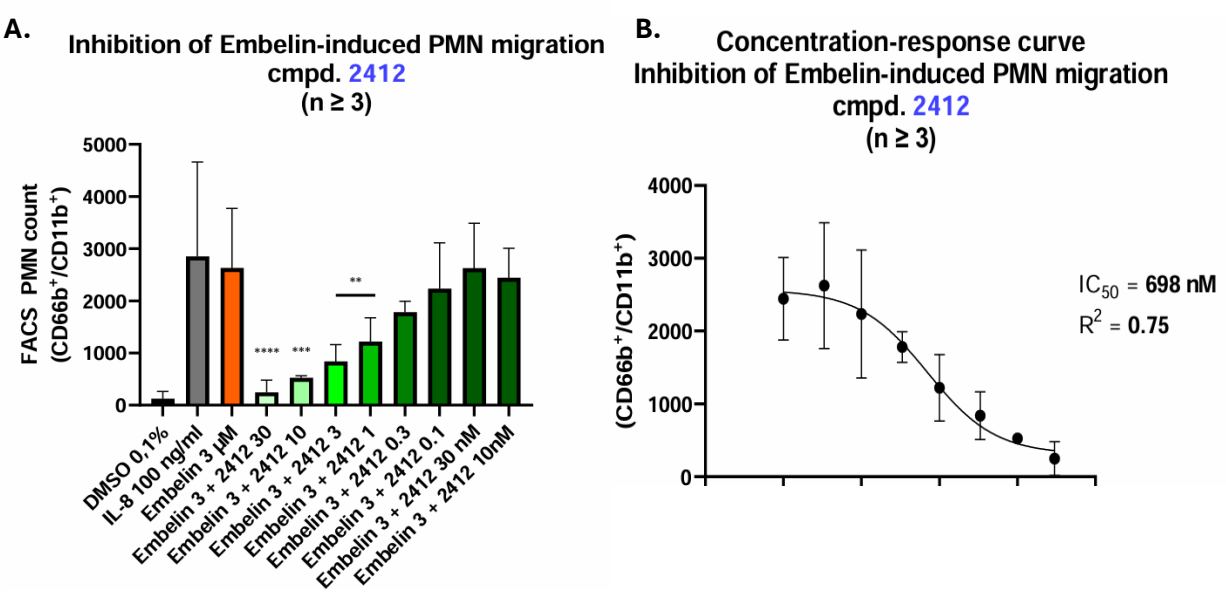


**Figure 32.** *Testing of different concentrations of compound 2412 in the PMN migration assay (A) and concentration-response curve (B).*

**(A)** To determine the statistical significance of the effects of compound 2412, the freshly isolated neutrophils were co-treated with different concentrations of 2412 ranging from 30 µM to 10 nM with Embelin (3 µM). The results of the tested compound are shown as mean values ± SD (standard deviation) of three biological replicates. The statistical analysis was performed by a one-way-ANOVA analysis. The negative control was DMSO 0.1% while IL-8 (100 ng/ml) and Embelin (3 µM) were used as a reference. [38]
Statistical significance evaluation: ****: $p \leq 0.0001$; ***: $p \leq 0.001$; **: $p \leq 0.01$; *: $p \leq 0.05$; ns: $p > 0.05$
**(B):** A concentration-dependent reduction of the migrated neutrophils by compound 2412 was determined in three independent measurements. The data is shown as the PMN count determined with neutrophil specific antibodies $CD66b^+/CD11b^+$ in FACS analysis. The software GraphPad Prism 6.01 was used for the nonlinear regression analysis to calculate an apparent $IC_{50}$ value of 698 nM (0.698 µM) with a $R^2$ value of 0.75. [38]

While the Embelin-induced GPR84-mediated PMN migration seems to be inhibited through Imbricaric acid, it was hypothesized that compound 2412 might also affect PMN migration induced by other chemoattractants. Therefore, IL-8, which induces neutrophil transmigration through CXCR1/2 activation independent of GPR84, was used as another control for the assay. [56,57] To test the theory, IL-8 (100 ng/ml) was used as a co-treatment with 2412 (30 µM) in three biological replicates. The results showed no statistically significant reduction of IL-8-induced neutrophil migration upon treatment with Imbricaric acid, indicating that the inhibitory effect was likely specific for GPR84-mediated signaling (**Figure 33**).

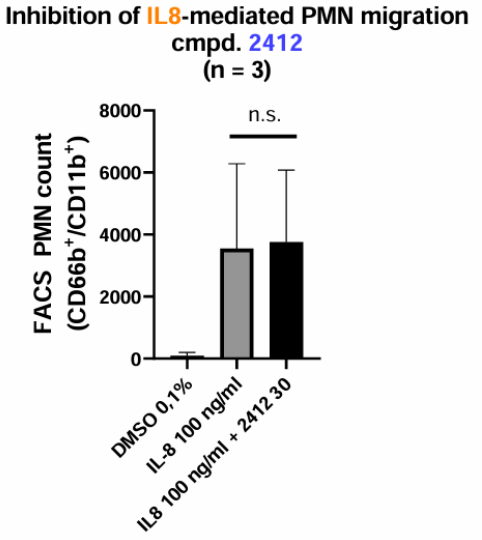


**Figure 33.** *Effect of compound 2412 on IL-8-mediated PMN migration.*

The freshly isolated neutrophils were co-treated with compound 2412 (30 µM) + IL-8 (100 ng/ml), to determine the potential ability of Imbricaric acid to inhibit IL-8-induced migration. The data of the tested co-treatment are shown as mean values ± SD (standard deviation) of three independent biological replicates. The statistical analysis was performed by one-way ANOVA analysis. The negative control was DMSO 0,1% while IL-8 (100 ng/ml) alone was used for comparison. [38]
Statistical significance evaluation: ns: $p > 0.05$

Further testing with this compound had to be halted due to its limited availability. The batch used for screenings in the EPAC assay, and migration assay had a verified purity of 99.39%. These findings suggest that Imbricaric acid is a potent inhibitor of GPR84-mediated PMN migration, validating it as a potential candidate for further pharmacological explorations.

### 3.1.4 Endocannabinoids

We then decided to investigate commercially available substances structurally related to Imbricaric acid. Olivetolic acid, a precursor for cannabinoid biosynthesis, was considered as a relevant candidate. In addition, two endocannabinoids, anandamide (AEA) and 2-arachidonylglycerol (2-AG), were screened in the PMN migration assay for their potential effect on neutrophils. [58] In addition to flow cytometry data to quantify neutrophils, images from the well of the 24-well plate were taken with the TECAN Spark® Microplate Reader before measurement. The visual inspections gave an insight into whether a reduction in neutrophil transmigration through the monolayer of Calu-3 cells was achieved.

It was observed in the assay that AEA did not inhibit neutrophil migration. On the contrary, 2-AG enhanced PMN migration resulting in an increase in cell count four times greater compared to Embelin at 3 µM (**Figure 34**).

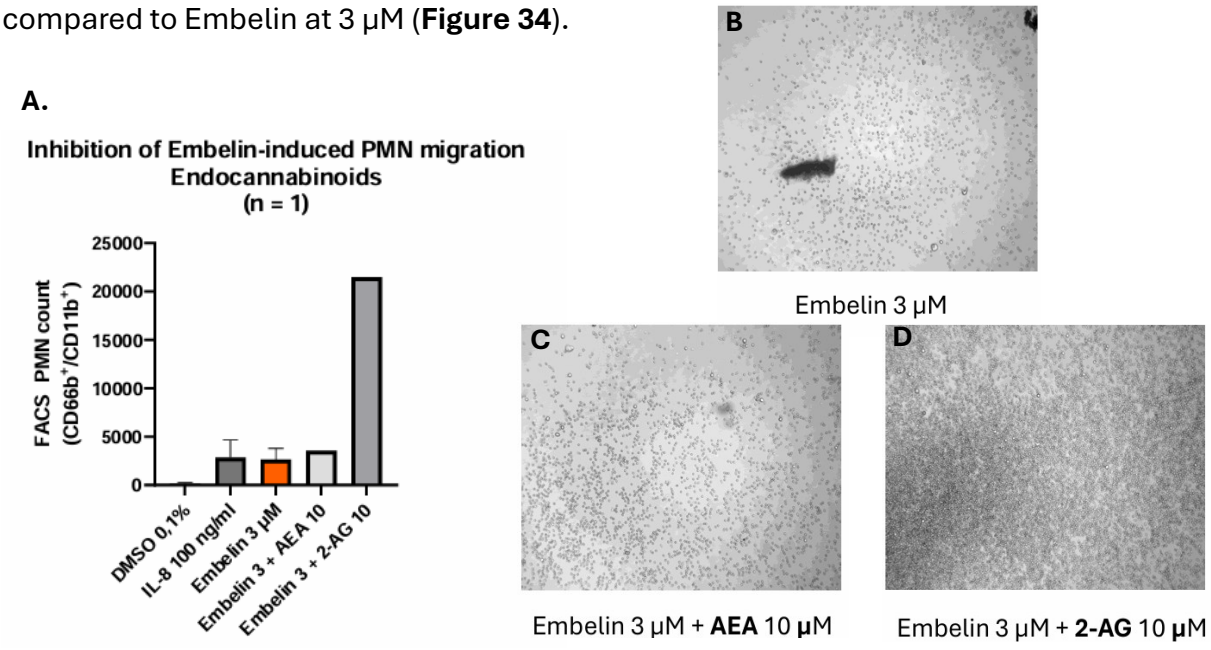


**Figure 34.** *Results of endocannabinoids in the PMN migration assay (A) and TECAN Spark® Microplate Reader well images (B-D).*

To assess whether endocannabinoids inhibited on Embelin-induced GPR84-mediated PMN migration, freshly isolated neutrophils were treated with anandamide (AEA 10 µM) and 2-arachidonoylglycerol (2-AG 10 µM) as a co-treatment with Embelin (3 µM). The bar graph shows results from one biological replicate; therefore, no statistical analysis was performed.
**(B)**: Well image of Embelin (3 µM) treated neutrophils after 2 hours of incubation
**(C)**: Well image of Embelin (3 µM) + AEA (10 µM) treated neutrophils after 2 hours of incubation
**(D)**: Well image of Embelin (3 µM) + 2-AG (10 µM) treated neutrophils after 2 hours of incubation

# E. Discussion

The second messenger cAMP plays an important role in cellular signaling pathways due to its involvement in multiple pathways concerning the regulation of inflammation, metabolism and other cellular functions. Intracellular cAMP levels are influenced by the binding of extracellular ligands to GPCRs. This activates adenylyl cyclase to transform ATP into cAMP. The focus of this study was on the receptors TGR5 and GPR84, due to their significance in multiple signaling pathways. [18,59] During this study, a variety of natural and synthetic compounds were screened in HEK293 cells to identify potential TGR5 agonists and GPR84 antagonists. A target-based screening employing a CRE-Luciferase assay was used for TGR5, while a two-step screening process was applied for the identification of GPR84 antagonists. First, the EPAC-FRET biosensor was used to assess potential compounds from the DNTI project by measuring the intracellular cAMP levels. Next, the promising candidates were tested for their ability to inhibit Embelin-induced GPR84-mediated PMN migration.

A limitation occurred during the screening process that applies to all assays involving the DNTI substances. These compounds had been stored at -70˚C since the DNTI project started in 2008, raising concerns about the degradation of chemical structures or possible contaminations caused by repeated freeze-thaw cycles. Additionally, the limited availability of some compounds, and attempts to obtain more were difficult since they were either not commercially available nor did the supplying laboratory provide more of them. This hindered further testing, especially for compound 2412 (Imbricaric acid).

## 1. G-protein coupled receptor TGR5

The first time a cAMP elevation was observed in the CRE-Luciferase assay was during an initial screening in which four flavonoids were identified as potential TGR5 agonists. Since flavonoids are well-known for their antibacterial, antioxidative, and anti-inflammatory properties, it was hypothesized that these compounds could also influence TGR5. [60–62]

After assessing 15 flavonoids from the DNTI project, it was revealed that, despite exhibiting TGR5-related activity this effect was not limited to this GPCR. The signaling patterns were similar in TGR5- and non-TGR5-expressing HEK cells, indicating that these compounds possess potential anti-inflammatory properties with no specific target that

could be identified in the performed assay. These findings further support the known role of flavonoids in influencing multiple anti-inflammatory responses. Although none of the compounds displayed specificity for TGR5, two flavonoids - compounds 2556 (3-Methoxynobiletin) and 2571, both polymethoxyflavones - did show a relative preference for the TGR5 signaling pathway. This indicates that this subclass of flavones could contain some potentially selective TGR5 agonists and should be further investigated. [63]

Interestingly, the hypothesis that gut-derived flavonoid metabolites could display agonistic behavior toward TGR5 was refuted during the screening. Although some metabolites tested in the CRE-Luciferase assay, such as syringic acid, which downregulates inflammation-related genes, or ferulic acid, which increases the growth of bacteria to produce short-chain fatty acids, have been studied for their anti-inflammatory properties, no effect was observed in the assay. All metabolites exhibited the same effect as the vehicle control (DMSO 0.1%), conveying that no direct influence of metabolites on TGR5 could be proven. [53–55]

Similar challenges were seen with leoligin derivatives 2823, 2826 and 2828. While compounds 2823 and 2826 exhibited modest TGR5 activity, derivative 2828 displayed a concentration-dependent activity with an estimated $EC_{50}$ of 17.3 µM. However, the results imply that any potential anti-inflammatory properties are not exclusively mediated via TGR5, due to the lack of TGR5 specificity of these compounds. In contrast, the previously studied derivative LT-188A displayed selective agonistic behavior towards TGR5 with no effect observed in non-TGR5-expressing cells or other bile acid receptors such as the Farnesoid X receptor (FXR). [64] Overall, these findings suggest that leoligin derivates may hold potential as TGR5 agonists, but the risk of off-target cAMP elevation should be considered.

## 2. G-protein coupled receptor GPR84

The identification of GPR84 antagonists involved a two-step process, compounds were first screened in the EPAC assay and sorted out if inactive before testing them in the PMN migration assay.

During the initial screening in the EPAC assay, it was observed that several compounds displayed elevated intracellular cAMP levels when tested at 30 µM. However, subsequent concentration-dependent experiments at 10 µM and 3 µM eliminated most candidates

due to a complete loss of activity at lower concentrations. Neolignane derivative 2815 exhibited notable activity, therefore, its evaluation was continued.

Compound 2815 exhibited a concentration-dependent activity with an $IC_{50}$ of 565.8 nM (0.566 µM). While evaluating 2815 for its GPR84 specificity, co-treatment with Forskolin (10 µM) alone revealed an increase of intracellular cAMP levels in non-GPR84-expressing cells, suggesting a possibility for off-target effects.

Upon testing compound 2815 in the PMN migration assay, the same effectiveness, which was observed in the EPAC assay, was not replicated. This may be due to the overexpression of the receptor in GPR84-expressing HEK cells compared to neutrophils which led to amplified signals from the compound in the EPAC assay.[65] Despite not exhibiting the desired results, compound 2815 could be used to conduct further research on structure-related GPR84 activity since other neolignane derivatives did not exhibit comparable activation. It should be compared to similar structures such as Honokiol and Magnolol, both known for their anti-inflammatory properties, which could help in identifying certain substitution patterns that promote GPR84 antagonism. [35,66–68]

In the follow-up experiments of four potential compounds for their inhibitory effects in the PMN migration assay, the neolignane derivative 2815 and the leoligin derivative 2819 were excluded from further testing due to their lack of inhibitory activity. This did not reflect their activity in the EPAC assay further decreasing their potential as antagonists. In contrast, the commercially available compound 1721 and the natural product 2412 (Imbricaric acid) could be confirmed as potent inhibitors Embelin-induced neutrophil migration. Interestingly, the results of the three replicates of compound 1721 varied significantly, especially the data of the third replicate, which questioned the reliability of the antagonistic effects. The cause of this remains unclear, despite evaluating the conditions of the assay repeatedly.

Compound 2412 (Imbricaric acid) was identified as the most promising candidate among the four tested substances. It demonstrated a significant reduction of Embelin-induced neutrophil migration at concentrations as low as 1 µM. Interestingly, it displayed no effect in the EPAC assay at concentrations ranging from 1 µM to 3 nM (data presented in the appendix, **Figure 38**). This inconsistency may be due to the use of different cell types (HEK cells versus neutrophils) which led to a difference in amplifying receptor signaling.[65,69]

To determine whether its inhibitory potential is GPR84-specific, Imbricaric acid was also tested against IL-8-mediated neutrophil migration. [57] However, it was observed that it did not significantly influence this signaling pathway further supporting its potential as a GPR84-specific antagonist.

Despite the benefits of additional testing, the limited compound availability halted further experiments. Efforts to obtain more substance were unsuccessful, as the original laboratory had no remaining stocks and the compound is not commercially available. The alternative approach to testing structurally related lichen compounds, such as olivetolic and evernic acid, were also hindered, due to commercial unavailability from the supplier.

Given these limitations, a different method was pursued to investigate similar mechanistic pathways. A previously published study focusing on biosynthetic engineering of cannabinoids from olivetolic acid, a structurally closely related lichen compound, led to the hypothesis that the endocannabinoids AEA and 2-AG might also affect this $G_i$-coupled receptor, thus interfering with the migration of neutrophils.[58] Interestingly, it was observed that rather than decreasing the migrated PMN count, both compounds seemed to increase it, with 2-AG showcasing the most pronounced effect, compared to the controls Embelin and IL-8. These findings suggest that 2-AG may possess pro-migratory properties possibly due to the structural similarities to known GPR84 agonists, for instance a long alkyl chain. [70]

Although more research on endocannabinoids as potential GPR84 agonists is needed, such interactions are unlikely to offer clinical benefits and are therefore from a therapeutic standpoint less relevant. Nonetheless, these findings do highlight the importance of structural patterns and GPR84 activation and could serve as the baseline for future structure-activity studies.

## F. Conclusion and Outlook

Identifying target-specific ligands for the GPCRs, TGR5 and GPR84, with *in vitro* anti-inflammatory properties proved to be a challenge as highlighted in this study. While the immune-modulatory responses are mediated through cAMP and ligand binding to GPCRs, several candidates, despite their promising activities, did not fulfill criteria such as target-specificity, compound stability, and availability.

For the TGR5 receptor, several compounds like flavonoids and leoligin derivatives were initially identified as agonists due to their induced cAMP elevation in the CRE-Luciferase assay, but with further concentration-dependent testing, the lack of target specificity became evident. These data suggest that the focus should be shifted from absolute target-specificity to selectivity for TGR5 compared to related receptors, such as FXR. [71,72]

In contrast, during the search for GPR84 antagonists, Imbricaric acid (compound 2412) emerged as a promising natural product in the EPAC assay. It also significantly reduced the GPR84-mediated migration of neutrophils. However, limited compound availability halted further evaluation. Inhibitory activity was also observed for compound 1721. Unfortunately, the inconsistent results from the third replicate questioned their reliability. Interestingly, both endocannabinoids seemed to increase PMN migration, which should be further investigated, even if the therapeutic value is unclear.

## G. References


1. Addis P, Bali U, Baron F, et al. Key aspects of modern GPCR drug discovery. SLAS Discov. 2024;29(1):1-22. doi:10.1016/j.slasd.2023.08.007
2. Ripoll L, von Zastrow M, Blythe EE. Intersection of GPCR trafficking and cAMP signaling at endomembranes. J. Cell Biol. 2025;224(4). doi:10.1083/JCB.202409027/277343
3. Hilger D, Masureel M, Kobilka BK. Structure and dynamics of GPCR signaling complexes. Nat. Struct. Mol. Biol. 2018;25(1):4. doi:10.1038/S41594-017-0011-7
4. Marsango S, Milligan G. Regulation of the pro-inflammatory G protein-coupled receptor GPR84. Br. J. Pharmacol. 2024;181(10):1500-1508. doi:10.1111/BPH.16098
5. Duboc H, Taché Y, Hofmann AF. The bile acid TGR5 membrane receptor: From basic research to clinical application. Dig. Liver Dis. 2014;46(4):302. doi:10.1016/J.DLD.2013.10.021
6. Müller-Esterl W. Biochemie. Eine Einführung Für Mediziner Und Naturwissenschaftler. 3rd ed. Springer Spektrum; 2018. p. 515-528
7. Dranoff G. Cytokines in cancer pathogenesis and cancer therapy. Nat. Rev. Cancer. 2004;4(1):11-22. doi:10.1038/nrc1252
8. Place DE, Kanneganti TD. The innate immune system and cell death in autoinflammatory and autoimmune disease. Curr. Opin. Immunol. 2020;67:95-105. doi:10.1016/j.coi.2020.10.013
9. Sherwood ER, Burelbach KR, McBride MA, et al. Brief Review: Innate Immune Memory and the Host Response to Infection. J. Immunol. 2022;208(4):785. doi:10.4049/jimmunol.2101058
10. Medina KL. Overview of the immune system. Handb. Clin. Neurol. 2016;133:61-76. doi:10.1016/b978-0-444-63432-0.00004-9
11. Parkin J, Cohen B. An overview of the immune system. Lancet. 2001;357(9270):1777-1789. doi:10.1016/S0140-6736(00)04904-7
12. In brief: The innate and adaptive immune systems - InformedHealth.org - NCBI Bookshelf [Internet]. Accessed June 4, 2025. https://www.ncbi.nlm.nih.gov/books/NBK279396/
13. Lämmermann T, Kastenmüller W. Concepts of GPCR-controlled navigation in the immune system. Immunol. Rev. 2019;289(1):205. doi:10.1111/imr.12752
14. Bröker BM, Fleischer B. Grundwissen Immunologie. 5th ed. Springer Spektrum (Springer-Verlag GmbH Deutschland); 2023. p. 68-126

15. Dong C. Cytokine Regulation and Function in T Cells. Annu. Rev. Immunol. 2021;39:51-76. doi:10.1146/annurev-immunol-061020-053702

16. Shi X, Cheng X, Jiang A, et al. Immune Checkpoints in B Cells: Unlocking New Potentials in Cancer Treatment. Adv. Sci.2024;11(47). doi:10.1002/advs.202403423

17. Kumar A, Watkins R, Vilgelm AE. Cell Therapy With TILs: Training and Taming T Cells to Fight Cancer. Front. Immunol. 2021;12:690499. doi:10.3389/fimmu.2021.690499

18. Robichaux WG, Cheng X. Intracellular cAMP Sensor EPAC: Physiology, Pathophysiology, and Therapeutics Development. Physiol. Rev. 2018;98(2):919. doi:10.1152/physrev.00025.2017

19. Futosi K, Fodor S, Mócsai A. Neutrophil cell surface receptors and their intracellular signal transduction pathways. Int. Immunopharmacol. 2013;17(3):638. doi:10.1016/j.intimp.2013.06.034

20. Wang S wei, Zhang Q, Lu D, et al. GPR84 regulates pulmonary inflammation by modulating neutrophil functions. Acta Pharmacol. Sin. 2023;44(8):1665-1675. doi:10.1038/s41401-023-01080-z

21. Perino A, Pols TWH, Nomura M, Stein S, Pellicciari R, Schoonjans K. TGR5 reduces macrophage migration through mTOR-induced C/EBPβ differential translation. J. Clin. Invest. 2014;124(12):5424. doi:10.1172/jci76289

22. Ye D, He J, He X. The role of bile acid receptor TGR5 in regulating inflammatory signalling. Scand. J. Immunol. 2024;99(4):e13361. doi:10.1111/sji.13361

23. van Nierop FS, Scheltema MJ, Eggink HM, et al. Clinical relevance of the bile acid receptor TGR5 in metabolism. Lancet Diabetes Endocrinol. 2017;5(3):224-233. doi:10.1016/S2213-8587(16)30155-3

24. Castellanos-Jankiewicz A, Guzmán-Quevedo O, Fénelon VS, et al. Hypothalamic bile acid-TGR5 signaling protects from obesity. Cell Metab. 2021;33(7):1483-1492.e10. doi:10.1016/j.cmet.2021.04.009

25. Pols TWH, Noriega LG, Nomura M, Auwerx J, Schoonjans K. The bile acid membrane receptor TGR5 as an emerging target in metabolism and inflammation. J. Hepatol. 2010;54(6):1263. doi:10.1016/j.jhep.2010.12.004

26. Kukk O, Klarenbeek J, Jalink K. Time-Domain Fluorescence Lifetime Imaging of cAMP Levels with EPAC-Based FRET Sensors. Methods Mol. Biol. 2022;2483:105-116. doi:10.1007/978-1-0716-2245-2_7

27. Guo C, Xie S, Chi Z, et al. Bile Acids Control Inflammation and Metabolic Disorder through Inhibition of NLRP3 Inflammasome. Immunity. 2016;45(4):802-816. doi:10.1016/j.immuni.2016.09.008

28. Pols TWH, Nomura M, Harach T, et al. TGR5 activation inhibits atherosclerosis by reducing macrophage inflammation and lipid loading. Cell Metab. 2011;14(6):747. doi:10.1016/j.cmet.2011.11.006

29. Aktar R, Rondinelli S, Peiris M. GPR84 in physiology—Many functions in many tissues. Br. J. Pharmacol. 2024;181(10):1524-1535. doi:10.1111/bph.16206

30. Abdel-Aziz H, Schneider M, Neuhuber W, et al. GPR84 and TREM-1 signaling contribute to the pathogenesis of reflux esophagitis. Mol. Med. 2015;21(1):1011-1024. doi:10.2119/molmed.2015.00098

31. Recio C, Lucy D, Purvis GSD, et al. Activation of the immune-metabolic receptor GPR84 enhances inflammation and phagocytosis in macrophages. Front. Immunol. 2018;9(JUN):1419. doi:10.3389/fimmu.2018.01419

32. Wang J, Wu X, Simonavicius N, Tian H, Ling L. Medium-chain fatty acids as ligands for orphan G protein-coupled receptor GPR84. J. Biol. Chem. 2006;281(45):34457-34464. doi:10.1074/jbc.M608019200

33. Forsman H, Dahlgren C, Mårtensson J, Björkman L, Sundqvist M. Function and regulation of GPR84 in human neutrophils. Br. J. Pharmacol. 2024;181(10):1536-1549. doi:10.1111/bph.16066

34. Storch U, Straub J, Erdogmus S, Gudermann T, Mederos y Schnitzler M. Dynamic monitoring of Gi/o-protein-mediated decreases of intracellular cAMP by FRET-based Epac sensors. Pflugers Arch. 2017;469(5):725. doi:10.1007/S00424-017-1975-1

35. Marsango S, Barki N, Jenkins L, Tobin AB, Milligan G. Therapeutic validation of an orphan G protein-coupled receptor: The case of GPR84. Br. J. Pharmacol. 2020;179(14):3529. doi:10.1111/bph.15248

36. Zhou Y, Meng J, Xu C, Liu J. Multiple GPCR Functional Assays Based on Resonance Energy Transfer Sensors. Front. Cell Dev. Biol. 2021;9:611443. doi:10.3389/fcell.2021.611443

37. Waltenberger B, Atanasov AG, Heiss EH, et al. Drugs from nature targeting inflammation (DNTI): A successful Austrian interdisciplinary network project. Monatsh. Chem. 2016;147(3):479-491. doi:10.1007/s00706-015-1653-y

38. Michels DM. Screening of natural products and derivatives for their influence on intracellular cAMP-levels for immunomodulation [master's thesis]. Vienna (Austria): University of Vienna; 2022.

39. Abaandou L, Quan D, Shiloach J. Affecting HEK293 Cell Growth and Production Performance by Modifying the Expression of Specific Genes. Cells. 2021;10(7):1667. doi:10.3390/cells10071667

40. Human Embryonic Kidney 293 [Internet]. Accessed June 12, 2025. https://www.beckman.at/resources/product-applications/lead-optimization/cell-line-development/human-embryonic-kidney-293

41. Protokoll Zelldissoziation mit Trypsin [Internet]. Accessed June 12, 2025. https://www.sigmaaldrich.com/AT/de/technical-documents/protocol/cell-culture-and-cell-culture-analysis/mammalian-cell-culture/cell-dissociation-with-trypsin

42. Kreft ME, Jerman UD, Lasič E, et al. The characterization of the human cell line Calu-3 under different culture conditions and its use as an optimized in vitro model to investigate bronchial epithelial function. Eur. J. Pharm. Sci. 2015;69:1-9. doi:10.1016/j.ejps.2014.12.017

43. Calu-3 Cells [Internet]. Accessed April 17, 2025. https://www.cytion.com/Calu-3-Cells/305032

44. GloResponse™ CRE-luc2P HEK293 Cell Line [Internet]. Accessed April 17, 2025. https://at.promega.com/en/products/luciferase-assays/genetic-reporter-vectors-and-cell-lines/gloresponse-cre-luc2p-hek293-cell-line/?catNum=E8500

45. Reddy K, Ramachandran B. A reproducible and affordable method of conducting luciferase assay. Anal. Biochem. 2024;692:115558. doi:10.1016/j.ab.2024.115558

46. Spergel DJ, Krüth U, Shimshek DR, Sprengel R, Seeburg PH. Using reporter genes to label selected neuronal populations in transgenic mice for gene promoter, anatomical, and physiological studies. Prog. Neurobiol. 2001;63(6):673-686. doi:10.1016/S0301-0082(00)00038-1

47. Verma AK, Noumani A, Yadav AK, Solanki PR. FRET Based Biosensor: Principle Applications Recent Advances and Challenges. Diagnostics. 2023;13(8):1375. doi:10.3390/diagnostics13081375

48. Gaidarov I, Anthony T, Gatlin J, et al. Embelin and its derivatives unravel the signaling, proinflammatory and antiatherogenic properties of GPR84 receptor. Pharmacol. Res. 2018;131:185-198. doi:10.1016/j.phrs.2018.02.021

49. Insel PA, Ostrom RS. Forskolin as a tool for examining adenylyl cyclase expression, regulation, and G protein signaling. Cell Mol. Neurobiol. 2003;23(3):305-314. doi:10.1023/a:1023684503883

50. Lahoz-Beneytez J, Elemans M, Zhang Y, et al. Human neutrophil kinetics: modeling of stable isotope labeling data supports short blood neutrophil half-lives. Blood. 2016;127(26):3431. doi:10.1182/blood-2016-03-700336

51. Axion Biosystems. What is TEER? [Internet]. Axion Biosystems; Accessed April 23, 2025. https://www.axionbiosystems.com/resources/video/what-teer

52. Srinivasan B, Kolli AR, Esch MB, Abaci HE, Shuler ML, Hickman JJ. TEER measurement techniques for in vitro barrier model systems. J. Lab. Autom. 2015;20(2):107. doi:10.1177/2211068214561025

53. Zhou M, Ma J, Kang M, et al. Flavonoids, gut microbiota, and host lipid metabolism. Eng. Life Sci. 2024;24(5). doi:10.1002/elsc.202300065

54. Baky MH, Elshahed M, Wessjohann L, Farag MA. Interactions between dietary flavonoids and the gut microbiome: a comprehensive review. Br. J. Nutr. doi:10.1017/S0007114521003627

55. Xie J, Xiong S, Li Y, et al. Phenolic acids from medicinal and edible homologous plants: a potential anti-inflammatory agent for inflammatory diseases. Front. Immunol. 2024;15:1345002. doi:10.3389/fimmu.2024.1345002

56. Dhayni K, Zibara K, Issa H, Kamel S, Bennis Y. Targeting CXCR1 and CXCR2 receptors in cardiovascular diseases. Pharmacol. Ther. 2022;237. doi:10.1016/j.pharmthera.2022.108257

57. Matsushima K, Yang D, Oppenheim JJ. Interleukin-8: An evolving chemokine. Cytokine. 2022;153:155828. doi:10.1016/j.cyto.2022.155828

58. Ma J, Gu Y, Xu P. Biosynthesis of cannabinoid precursor olivetolic acid in genetically engineered Yarrowia lipolytica. Commun. Biol. 2022;5(1). doi:10.1038/S42003-022-04202-1

59. Sassone-Corsi P. The Cyclic AMP pathway. Cold Spring Harb Perspect. Biol. 2012;4(12). doi:10.1101/cshperspect.a011148

60. Serafini M, Peluso I, Raguzzini A. Flavonoids as anti-inflammatory agents. Proc. Nutr. Soc. 2010;69(3):273-278. doi:10.1017/S002966511000162X

61. Slika H, Mansour H, Wehbe N, et al. Therapeutic potential of flavonoids in cancer: ROS-mediated mechanisms. Biomed. Pharmacother. 2022;146:112442. doi:10.1016/j.biopha.2021.112442

62. Shen N, Wang T, Gan Q, Liu S, Wang L, Jin B. Plant flavonoids: Classification, distribution, biosynthesis, and antioxidant activity. Food Chem. 2022;383:132531. doi:10.1016/j.foodchem.2022.132531

63. Gan R, Liu Y, Li H, et al. Natural sources, refined extraction, biosynthesis, metabolism, and bioactivities of dietary polymethoxyflavones (PMFs). Food Sci. Hum. Wellness. 2024;13(1):27-49. doi:10.26599/fshw.2022.9250003

64. Perhal AF, Schwarz PF, Linder T, Mihovilovic MD, Schnürch M, Dirsch VM. Identification and Characterization of a Leoligin-Inspired Synthetic Lignan as a TGR5 Agonist. J. Nat. Prod. 2025;88(4). doi:10.1021/acs.jnatprod.5c00059

65. Kenakin TP. Chapter 6 - Agonists: the measurement of affinity and efficacy in functional assays. In: Kenakin TP, ed. A Pharmacology Primer. 6th ed. Academic Press; 2022:151-188.

66. Hua KF, Hsu HT, Huang MS, et al. Honokiol Exhibits Anti-NLRP3 Inflammasome and Antimicrobial Properties in Neisseria gonorrhoeae-Infected Macrophages. J. Inflamm. Res. 2024;17:3499. doi:10.2147/jir.s454221

67. Zálešák F, Bon DJYD, Pospíšil J. Lignans and Neolignans: Plant secondary metabolites as a reservoir of biologically active substances. Pharmacol. Res. 2019;146:104284. doi:10.1016/j.phrs.2019.104284

68. Chiu KC, Shih YH, Wang TH, et al. In vitro antimicrobial and antipro-inflammation potential of honokiol and magnolol against oral pathogens and macrophages. J. Formos. Med. Assoc. 2021;120(2):827-837. doi:10.1016/j.jfma.2020.09.002

69. Kenakin TP. Chapter 2 - How different tissues process drug response. In: Kenakin TP, ed. A Pharmacology Primer 6th ed. Academic Press; 2022:23-45.

70. Chouinard F, Lefebvre JS, Navarro P, et al. The Endocannabinoid 2-Arachidonoyl-Glycerol Activates Human Neutrophils: Critical Role of Its Hydrolysis and De Novo Leukotriene B4 Biosynthesis. J. Immunol. 2011;186(5):3188-3196. doi:10.4049/jimmunol.1002853

71. Chiang JYL, Pathak P, Liu H, Donepudi A, Ferrell J, Boehme S. Intestinal FXR and TGR5 signaling in metabolic regulation. Dig. Dis. 2017;35(3):241. doi:10.1159/000450981

72. Chiang JYL, Ferrell JM. Bile acid receptors FXR and TGR5 signaling in fatty liver diseases and therapy. Am. J. Physiol. Gastrointest. Liver Physiol. 2020;318(3):G554. doi:10.1152/ajpgi.00223.2019

73. CAS SciFinder [Internet]. Accessed June 13, 2025. https://scifinder-n.cas.org.

# H. Appendix

## 1. Abbreviations

| | | |
|---|---|---|
| A | 2-AG | 2-Arachidonoylglycerol |
| | AC | Adenylyl cyclase |
| | AEA | Anandamide |
| | AKT | Protein Kinase B |
| | ALI | Acute lung injury |
| | APC | Antigen presenting cell |
| B | BALF | Bronchoalveolar lavage fluid |
| | BCR | B cell receptor |
| C | cAMP | Cyclic adenosine monophosphate |
| | CFP | Cyan fluorescent protein |
| | CM | Complete medium |
| | CRE | cAMP responsive element |
| | CREB | cAMP responsive element binding protein |
| | CRE-Luc. | cAMP responsive element-Luciferase |
| D | DC | Dendritic cell |
| | $ddH_2O$ | Double distilled water |
| | DMEM | Dulbecco's Modified Eagle Medium |
| | DMEM/F-12 | Dulbecco's Modified Eagle Medium + F-12 - nutrient mixture |
| | DMSO | Dimethyl sulfoxide |
| | DNTI | Drugs from nature targeting inflammation |
| | DSS | Dextran sulfate sodium |
| | DTT | Dithiothreitol |
| E | $EC_{50}$ | Half maximal effective concentration |
| | EDTA | Ethylenediaminetetraacetic acid |
| | EPAC | Exchange protein directly activated by cAMP |

| | | |
|---|---|---|
| F | FACS | Fluorescence activated cell sorting |
| | FBS | Fetal bovine serum |
| | FRET | Förster resonance energy transfer |
| | FXR | Farnesoid X receptor |
| G | GDP | Guanosine diphosphate |
| | GLP-1 | Glucagon like protein 1 |
| | GPBAR 1 | G-protein coupled bile acid receptor 1 |
| | GPCR | G-protein coupled receptor |
| | GPR84 | G-protein coupled receptor 84 |
| | G-protein | Guanine nucleotide-binding protein |
| | GTP | Guanosine triphosphate |
| H | HBS | HEPES-buffered-saline |
| | HEK293 | Human embryonic kidney 293 cells |
| | HEPES | 4-(2-hydroxyethyl)-1-piperazineethanesulfonic acid |
| I | $IC_{50}$ | Half-maximal inhibitory concentration |
| | IL-1 | Interleukin 1 |
| | IL-18 | Interleukin 18 |
| | IL-1β | Interleukin 1β |
| | IL-6 | Interleukin 6 |
| L | LCA | Lithocholic acid |
| | LDL | Low density lipoprotein |
| | LIP | Liver inhibitory protein |
| | LPS | Lipopolysaccharide |
| M | MCFA | Medium-chain fatty acid |
| | MHC | Major histocompatibility complex |
| N | NF-κB | Nuclear factor kappa-B |
| | NLRP3 | NOD-like receptor protein 3 |
| | NP | Natural product |

| | | |
|---|---|---|
| P | PAMP | Pathogen-associated molecular patterns |
| | PBS | Phosphate-buffered saline |
| | PI | Propidium iodide |
| | PKA | Protein Kinase A |
| | PLC | Phospholipase C |
| | PMN | Polymorphonuclear neutrophil |
| | PRR | Pattern recognition receptor |
| R | RBC | Red blood cell |
| | RPMI | Roswell Park Memorial Institute |
| S | SD | Standard deviation |
| | SM | Stripped medium |
| | STAT1 | Signal transducer and activator of transcription 1 |
| T | TGR5 | Takeda G-protein receptor 5 |
| | TCR | T cell receptor |
| | Th1 | T helper cell 1 |
| | Th2 | T helper cell 2 |
| | TNFα | Tumor necrosis factor α |

## 2. Figures

# 3. Tables

# 4. Viability data of CRE-Luciferase assays

## 4.1 Viability from the initial CRE-Luciferase screening in TGR5 HEK cells

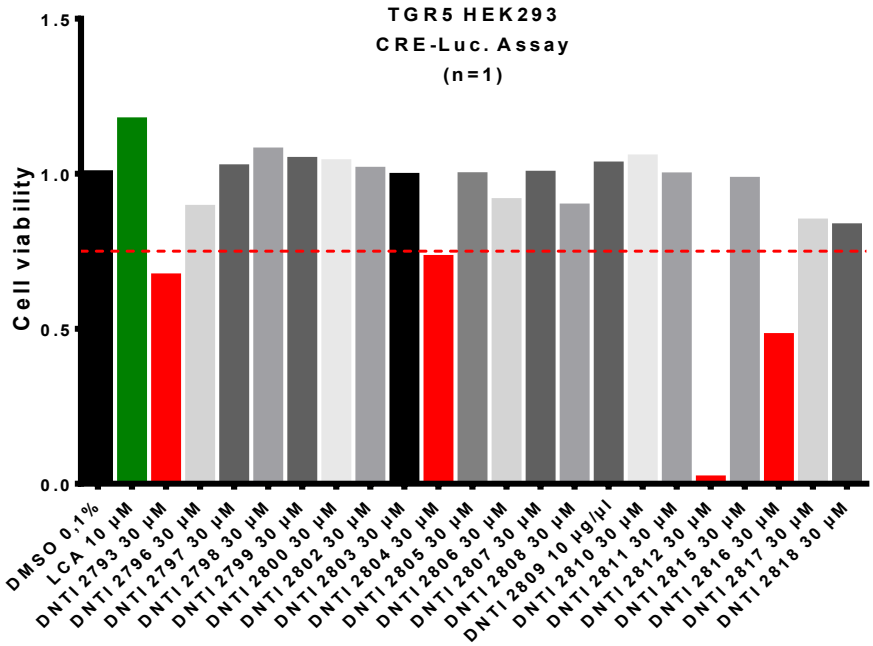


**Figure 35**. *Viability data of compounds 2793-2818 in TGR5 HEK cells during CRE-Luciferase assay.*

In the graph the cell viability of compounds 2793 to 2818, which were measured during CRE-Luciferase assay, are displayed. The measurement was conducted through GFP fluorescence, a parameter substituting for viability. The aim was to achieve a viability higher than 0,75 for the compounds to be non-cytotoxic. The red marked bars highlight compounds under the given limit. The green marked bar highlights the positive control LCA (10 µM). [38]
**DMSO** = Dimethyl sulfoxide, **DNTI** = Drugs from nature targeting inflammation, **LCA** = Lithocholic acid

## 4.2 Viability data of microbial metabolites in TGR5 HEK cells

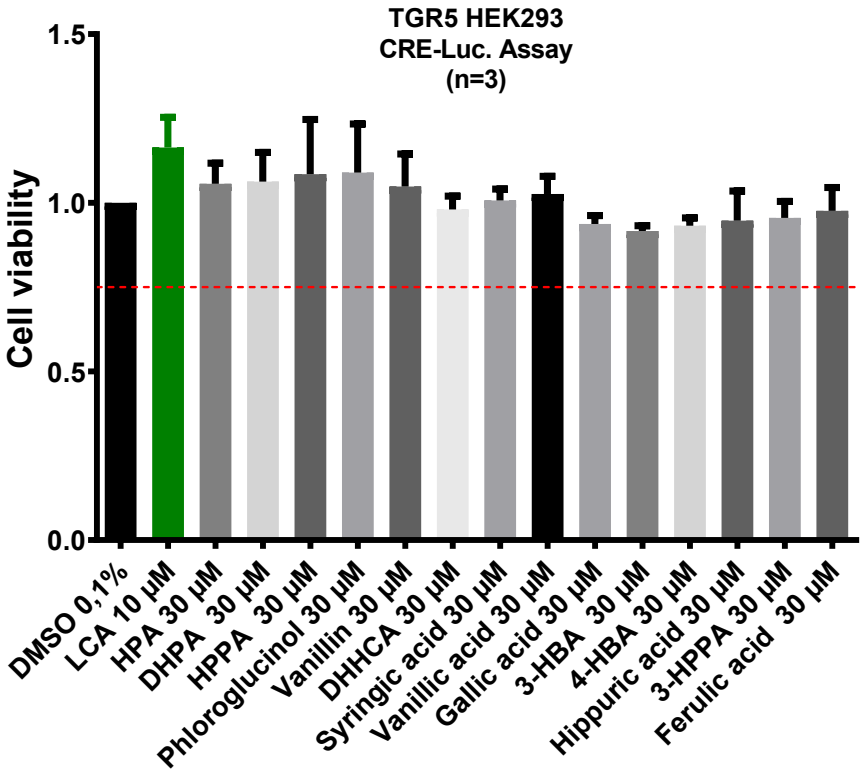


**Figure 36.** *Viability results of flavonoid metabolites in TGR5 expressing cells in CRE-Luciferase assay.*

In the graph the cell viability of the tested metabolites , which were measured during CRE-Luciferase assay, are displayed. The measurement was conducted through GFP fluorescence, a parameter substituting for viability. The aim was to achieve a viability higher than 0,75 for the compounds to be non-cytotoxic. The results of the tested compound are shown as mean values ± SD (standard deviation) of three biological replicates measured in technical quadruplicates. The green marked bar highlights the positive control LCA (10 µM). [38]

**DMSO** = Dimethyl sulfoxide, **LCA** = Lithocholic acid, **HPA** = 3- Hydroxyphenylacetic acid, **DHPA** = 3,4-Dihydroxyphenylacetic acid, **HPPA** = 3-(4-Hydroxyphenyl)propionic acid, **DHHCA** = 3,4-Dihydroxyhydrocinnamic acid, **3-HBA** = 3-Hydroxybenzoic acid, **4-HBA** = 4-Hydroxybenzoic acid, **3-HPPA** = 3-(3-Hydroxyphenyl)propionic acid

## 4.3 Viability data from the CRE-Luciferase assay in TGR5 HEK cells

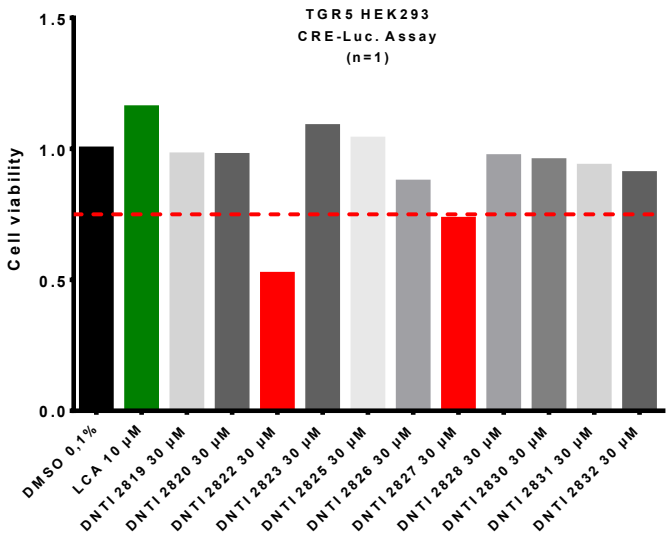


**Figure 37.** *Viability data of compounds 2819 to 2832 in TGR5 HEK cells during CRE-Luciferase assay.*

In the graph the cell viability of compounds 2819-2832, which were measured during CRE-Luciferase assay, are displayed. The measurement was conducted through GFP fluorescence, a parameter substituting for viability. The aim was to achieve a viability higher than 0,75 for the compounds to be non-cytotoxic. The red marked bars highlight compounds under the given limit. The green marked bar highlights the positive control LCA (10 µM). [38]
**DMSO** = Dimethyl sulfoxide, **DNTI** = Drugs from nature targeting inflammation, **LCA** = Lithocholic acid

## 5. Devices used for assays

*Table 6. Used devices for all assays.*

| Device | Assays | Source |
|---|---|---|
| HERAsafe®KS18 | EPAC<br>CRE-Luciferase<br>PMN Migration | Thermo Fisher Scientific Inc. (Waltham, CA, USA) |
| Julabo® SW23 | EPAC<br>CRE-Luciferase<br>PMN Migration | Julabo GmbH (Allentown, PA, USA) |
| HERAcell® 150 Incubator | EPAC<br>CRE-Luciferase<br>PMN Migration | Thermo Fisher Scientific Inc. (Waltham, CA, USA) |
| Olympus CKX31 Light Microscope | EPAC<br>CRE-Luciferase<br>PMN Migration | Olympus Europa GmbH (Hamburg, Germany) |
| Centrifuge Heraeus™ Multifuge 1 S-R | EPAC<br>CRE-Luciferase<br>PMN Migration | Thermo Fisher Scientific Inc. (Waltham, CA, USA) |
| ViCell™ XR Cell Viability Analyzer | EPAC<br>CRE-Luciferase<br>PMN Migration | Beckmann Coulter (Fullerton, CA, USA) |
| VM-3000 Mini Vortexer | EPAC<br>CRE-Luciferase<br>PMN Migration | VWR International (Radnor, PA, USA) |
| TECAN Spark® Microplate Reader | EPAC<br>CRE-Luciferase<br>PMN Migration | Tecan Group Ltd. (Maennedorf, Switzerland) |
| Multi-MicroPlate Genie™ shaker | CRE-Luciferase | Scientific Industries (New York, USA) |
| MACSQuant® Analyzer 10 Flow Cytometer | PMN Migration | Miltenyi Biotech (Gladbach, Germany) |
| Heraeus™ Fresco 21 Centrifuge | PMN Migration | Thermo Fisher Scientific Inc. (Waltham, CA, USA) |

## 6. Flavonoids screened in the CRE-Luciferase assay

*Table 7. CAS Registry Number of flavonoid structures shown in **Figure 3**.*

| Flavonoids with DNTI number | CAS Registry Number |
|---|---|
| Tricin (DNTI 1682) | 520-32-1 |
| Salvigenin (DNTI 1696) | 19103-54-9 |
| Oroxylin A (DNTI 1950) | 480-11-5 |
| Chrysin (DNTI 1951) | 480-40-0 |
| Baicalein (DNTI 1952) | 491-67-8 |
| Hispidulin (DNTI 1953) | 1447-88-7 |
| 3-Methoxynobiletin (DNTI 2556) | 1178-24-1 |
| DNTI 2571 | 98007-03-5 |
| Pectolinarigenin (DNTI 2572) | 520-12-7 |
| DNTI 2573 | 2569-77-9 |
| Kaempferol (DNTI 2796) | 520-18-3 |
| Hesperetin (DNTI 2797) | 520-33-2 |
| Naringenin (DNTI 2798) | 480-41-1 |
| DNTI 2799 | 326795-05-5 |
| 7-Methylaromadendrin (DNTI 2800) | 37971-69-0 |
| Flavone (core structure) | 525-82-6 |
| Flavanone (core structure) | 487-26-3 |

## 7. Flavonoid metabolites screened in the CRE-Luciferase assay

*Table 8.Screened microbial metabolites in CRE-Luciferase.*

| Compounds | Source |
|---|---|
| 3- Hydroxyphenylacetic acid (HPA) | Carl-Roth (Karlsruhe, Germany) |
| 3,4-Dihydroxyphenylacetic acid (DHPA) | Carl-Roth (Karlsruhe, Germany) |
| 3-(4-Hydroxyphenyl)propionic acid (HPPA) | Carl-Roth (Karlsruhe, Germany) |
| Phloroglucinol | Carl-Roth (Karlsruhe, Germany) |
| Vanillin | Carl-Roth (Karlsruhe, Germany) |
| 3,4-Dihydroxyhydrocinnamic acid (DHHCA) | Carl-Roth (Karlsruhe, Germany) |
| Syringic acid | Carl-Roth (Karlsruhe, Germany) |
| Vanillic acid | Carl-Roth (Karlsruhe, Germany) |
| Gallic acid | Carl-Roth (Karlsruhe, Germany) |
| 3-Hydroxybenzoic acid (3-HBA) | Carl-Roth (Karlsruhe, Germany) |
| 4- Hydroxybenzoic acid (4-HBA) | Carl-Roth (Karlsruhe, Germany) |
| Hippuric acid | Carl-Roth (Karlsruhe, Germany) |
| 3-(3-Hydroxyphenyl)propionic acid (3-HPPA) | Carl-Roth (Karlsruhe, Germany) |
| Ferulic acid | Carl-Roth (Karlsruhe, Germany) |

# 8. Results of compound 2412 in the EPAC assay

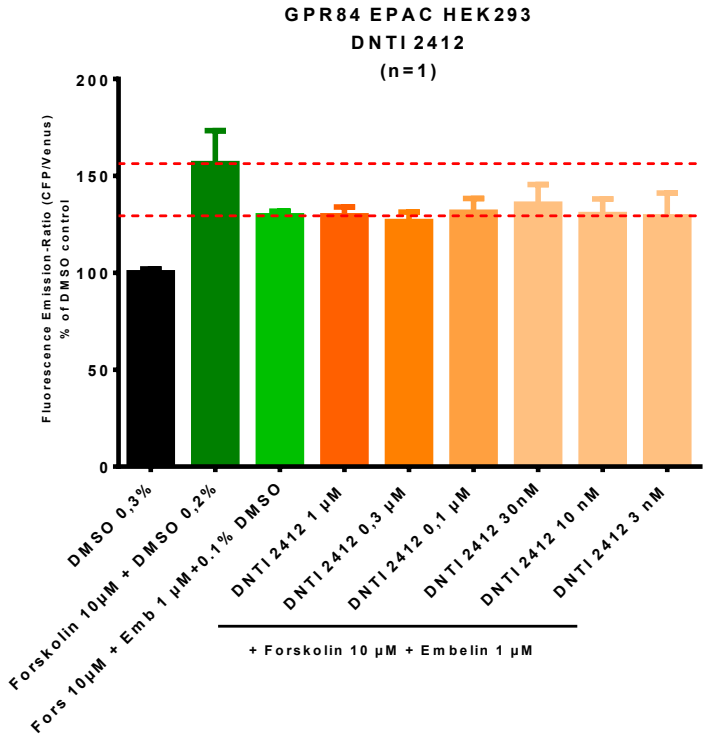


**Figure 38.** *Screening results from DNTI 2412 at concentrations 1 µM to 3 nM in the EPAC assay.*

The bar graph displays the evaluated activity of Imbricaric acid (compound 2412) at lower concentrations in the EPAC assay. As seen in the graph, the compound did not increase intracellular cAMP levels compared to control Forskolin (10 µM). This suggests that no influence on GPR84 was observed at concentrations ranging from 1 µM to 3 nM.

**DMSO** = Dimethyl sulfoxide, **DNIT** = Drugs from nature targeting inflammation, **Fors** = Forskolin, **Emb** = Embelin